Long-term and seasonal variations in the levels of hydrogen peroxide, methylhydroperoxide, and selected compounds over the Pacific Ocean

D. W. O'Sullivan,[1] B. G. Heikes,[2] J. Snow,[2] P. Burrow,[1] M. Avery,[3] D. R. Blake,[4] G. W. Sachse,[5] R. W. Talbot,[6] D. C. Thornton,[7] and A. R. Bandy[7]

Received 15 April 2003; revised 24 July 2003; accepted 21 August 2003; published 1 July 2004.

[1] The National Aeronautics and Space Administration's Global Tropospheric Experiment program has conducted five sampling programs examining the Pacific troposphere from 1991 to 2001. Flights on two aircraft, a P3-B and DC-8, sampled the Pacific troposphere at altitudes from 0.5 km to 13 km and from 130°E to 115°W and from 65°N to 70°S. Long-term trends in the observed species mixing ratios in different geographic regions are presented. Changes in species mixing ratios are discussed with respect to changes in source, transport, and photochemical production and loss processes over the decade study period. CH_4 and CO_2 exhibited average annual mixing ratio increases of 6.39 ppbv yr^{-1} and 1.92 ppmv yr^{-1}, respectively. O_3, CO, and NO all exhibit significantly higher mixing ratios in the north Pacific troposphere in the spring than in the fall. However, there is no clear annual trend for these species. H_2O_2 mixing ratios were 38 ± 16% higher (Δ(fall−spring) 258 ± 34 pptv), and CH_3OOH was 61 ± 15% higher (Δ343 ± 76 pptv) throughout the Pacific troposphere in the fall than in the spring. During 2001, SO_2 loading in the North Pacific is 2–3 times larger than during earlier years. Anthropogenic tracer gases, C_2H_6, C_3H_8, C_2H_2, and C_2Cl_4, do not exhibit comparable increases in their average mixing ratios during the decade study period. CH_3I, a tracer for oceanic emission, also does not exhibit an increase in 2001. Sulfur loading characterized by SO_2 also does not exhibit a clear annual trend. The enhanced sulfur loading during 2001 appears to have resulted in a suppression of H_2O_2 mixing ratios in the lower troposphere throughout the midlatitude North Pacific. *INDEX TERMS:* 0317 Atmospheric Composition and Structure: Chemical kinetic and photochemical properties; 0322 Atmospheric Composition and Structure: Constituent sources and sinks; 0365 Atmospheric Composition and Structure: Troposphere—composition and chemistry; 0368 Atmospheric Composition and Structure: Troposphere—constituent transport and chemistry; *KEYWORDS:* peroxides, distributions, troposphere

Citation: O'Sullivan, D. W., B. G. Heikes, J. Snow, P. Burrow, M. Avery, D. R. Blake, G. W. Sachse, R. W. Talbot, D. C. Thornton, and A. R. Bandy (2004), Long-term and seasonal variations in the levels of hydrogen peroxide, methylhydroperoxide, and selected compounds over the Pacific Ocean, *J. Geophys. Res.*, *109*, D15S13, doi:10.1029/2003JD003689.

1. Introduction

[2] The distributions of hydrogen peroxide (H_2O_2), methylhydroperoxide (CH_3OOH), SO_2, DMS, O_3, CO, CO_2, selected hydrocarbons, and selected nitrogen containing species have been observed in the oceanic troposphere during NASA's Global Tropospheric Experiment (GTE) program. Over the last 10 years this program sponsored five field campaigns in which the peroxide and many other species mixing ratios were determined over the Pacific Ocean (Table 1). The first was the Pacific Exploratory Mission (PEM), West A (PWA) where measurements were made in the western Pacific from the NASA DC-8 during September and October of 1991. The second phase of the Pacific Exploratory Mission West B (PWB) occurred in January and February of 1993. In September and October of 1996, PEM Tropics A (PTA) occurred and focused on the tropical Pacific troposphere involving both the NASA DC-8 and P3-B aircraft. PTA was followed by a second tropical Pacific mission, PEM Tropics B (PTB), which sampled the troposphere during March and April of 1999. The most recent mission focused on examining the Transport and Chemical Evolution over the Pacific (TRACE-P (TRP)) of Asian outflow during March and April of 2001 [*Jacob et al.*, 2003]. The following special

[1]Chemistry Department, U.S. Naval Academy, Annapolis, Maryland, USA.
[2]Center for Atmospheric Chemical Studies, Graduate School of Oceanography, University of Rhode Island, Narragansett, Rhode Island, USA.
[3]Atmospheric Sciences Division, NASA Langley Research Center, Hampton, Virginia, USA.
[4]Department of Chemistry, University of California, Irvine, California, USA.
[5]NASA Langley Research Center, Hampton, Virginia, USA.
[6]Institute for the Study of Earth, Oceans, and Space, University of New Hampshire, Durham, New Hampshire, USA.
[7]Department of Chemistry, Drexel University, Philadelphia, Pennsylvania, USA.

0148-0227/04/2003JD003689$09.00

Table 1. NASA GTE Mission Dates and Aircraft Used

GTE Missions	Dates	Aircraft
Pacific Exploratory Mission West A (PWA)	September–October 1991	DC8
Pacific Exploratory Mission West B (PWB)	February–March 1994	DC8
Pacific Exploratory Mission Tropics A (PTA)	August–October 1996	DC8 and P3B
Pacific Exploratory Mission Tropics B (PTB)	February–April 1999	DC8 and P3B
Transport and Chemical Evolution over the Pacific (TRP)	February–April 2001	DC8 and P3B

section papers contribute to the principal goals of enhancing our understanding of the distribution of O_3 over the Pacific Ocean through an exploration of atmospheric composition and dynamics and, second, improving our understanding of sulfur gas chemistry in the Pacific troposphere: "Pacific Exploratory Mission-West Phase A" (*Journal of Geophysical Research*, *101*(D1), 1641–2147, 1996), "Pacific Exploratory Mission-West, Phase B" (*Journal of Geophysical Research*, *102*(D23), 28,223–28,671, 1997), "Pacific Exploratory Mission-Tropics A (PEM-Tropics A)" (*Journal of Geophysical Research*, *104*(D5), 5565–5876, 1999), and "NASA Global Tropospheric Experiment Pacific Exploratory Mission in the Tropics Phase B, Part 1: Measurements and Analysis (PEM-Tropics B)" (*Journal of Geophysical Research*, *106*(D23), 32,401–34,776, 2001).

[3] Long-term changes in the levels of gas phase species in the atmosphere can be driven by a variety of processes. First, if the compound is directly emitted by anthropogenic activity, changes in the level or geographic location of the anthropogenic activity can have a significant effect on the regional distribution. Second, if a target compound is photochemically produced in the atmosphere, changes in precursor source emission characteristics can affect photochemical production. Additionally, changes in levels of compounds that compete with a specific formation or loss process for the target species may impact the observed levels of the target compound. Finally, shifts from one meteorological regime to another may alter the transport path for compounds, changing their regional distributions. Meteorological regime shifts may also change deposition and heterogeneous processes that are typical of a particular meteorological pattern. For example, the presence and intensity of El Niño can affect the regional meteorology in the Pacific troposphere. Understanding the long-term changes or loading of a compound in the atmosphere requires knowledge of all of these different processes. An additional complication in establishing the long-term trend for a species is appropriately accounting for the effects introduced by a sampling bias, for example, sampling in a limited number of seasons. Most of the GTE missions occurred during either Northern Hemisphere spring or fall, when species with seasonal cycles exhibit the greatest rate of change in ambient levels. Consequently, a shift of a few weeks in time can make a large difference in the observed ambient levels. Unequivocally determining whether observed differences in species mixing ratios between field programs are due to a long-term trend or due to a few weeks difference in the sampling window between programs, is a challenging endeavor. However, understanding the chemical evolution of the troposphere over long time periods is necessary to evaluate pollution and chemical loading trends. It is equally important to determine if any changes in loading locally are altering levels of compounds on a regional spatial scale.

[4] To address these questions, we have examined the mean mixing ratios of a variety of compounds in different regions of the Pacific troposphere from 1991 to 2001. In this paper we present the decadal changes in the levels of H_2O_2, CH_3OOH, and selected species in different regions of the Pacific troposphere during the GTE field campaigns. Sample collection and analytical procedures for the peroxides are briefly described for the PTB and TRP missions, as well as the data sets used in the compilation. Trends in species mixing ratios are presented and the influence of changes in emission, photochemical production/loss, and transport regimes are explored.

2. Experiment

2.1. Data Compilation From the Field Missions

[5] The GTE field programs involved measurements of a number of chemical species, which contribute to understanding the chemistry of O_3 and SO_2 in the troposphere [*Raper et al.*, 2001]. A number of these measurements were used to interpret the observed changes in peroxide distributions. Since each of the instruments in the aircraft payload for the various missions had a unique sampling and analysis cycle, their respective measurements were merged to the peroxide time base for the early missions, PWA, PWB, and PTA, nominally 5 min. For the PTB and the TRP missions, the data were merged to a 5-min time base. Observations from instruments with a shorter time resolution than the peroxide measurements were averaged over the peroxide analysis cycle. If a species was not directly measured during the peroxide sample interval, it was treated as missing. If a species sample interval exceeded the peroxide sample interval, the species concentration was assumed to remain constant in the data merge for multiple peroxide sample intervals.

[6] The data for each mission were geographically partitioned into eight regions. The high-latitude north Pacific (HLNP) region was composed of all data with sampling latitude >45°N. A similar high-latitude south Pacific (HLSP) region was also used for all data obtained at latitudes >45°S. This region was only sampled during PTA by the DC-8 and is represented by data from only two flights. The troposphere over the Pacific Ocean was partitioned into east and west regions at the date line: East Pacific (EP) is composed of data with longitudes >90° and <180°; west Pacific (WP) data have longitudes >180° and <250°. Midlatitude north Pacific (MN) extended from 10° to 45°N, the equatorial region (EQ) extended from 5°S to 10°N, and the midlatitude south pacific (MS) region is composed of data from 5°S to 45°S. The latitude and longitude divisions are combined to generate a specific

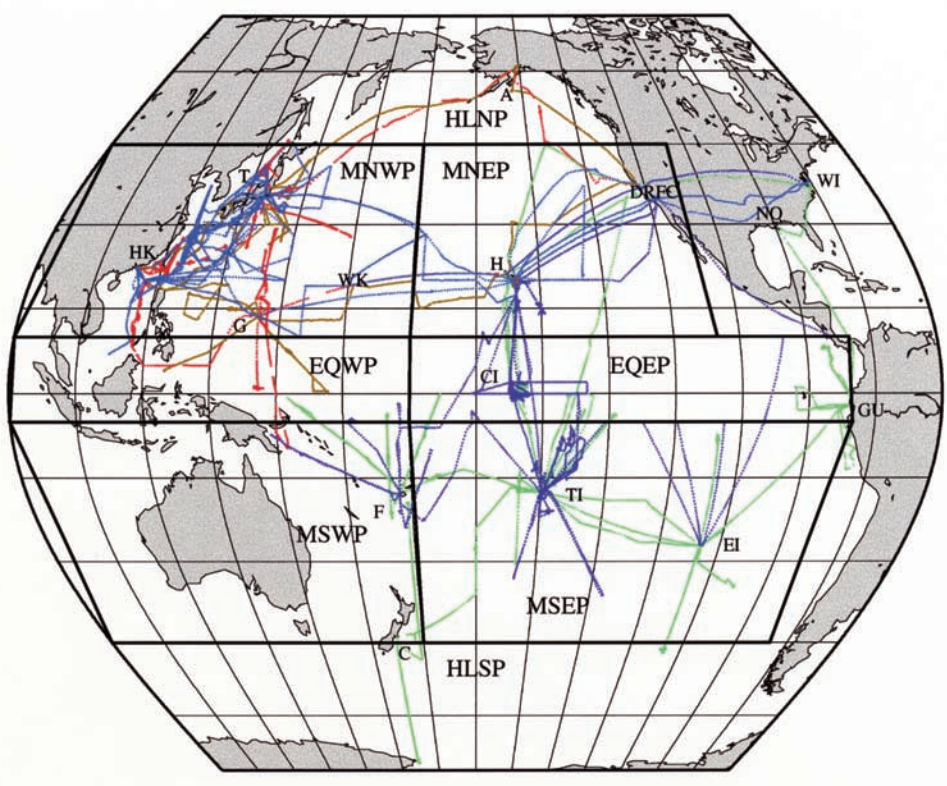

Figure 1. Flight tracks for the GTE Pacific Exploratory Missions. PWA is in gold, PWB is in red, PTA is in green, PTB is in magenta, and TRP is in blue. Abbreviations are as follows: A, Anchorage; C, Christchurch; CI, Christmas Island; DFRC, Dryden Flight Research Center; EI, Easter Island; F, Fiji; G, Guam; GU, Guayaquil; H, Honolulu; HK, Hong Kong; NO, New Orleans; T, Tokyo; TI, Tahiti; WI, Wallops Island; and WK, Wake Island.

region, for example, the midlatitude northeastern Pacific (MNEP) (Figure 1).

2.2. Peroxide Analytical Methods and Trace Gas Figures of Merit

[7] Gas phase H_2O_2 and CH_3OOH were collected with continuous flow glass cyclone separators [*Lazrus et al.*, 1986] and quantified using the high-performance liquid chromatographic (HPLC) fluorometric method described by *Lee et al.* [1995] and *Kok et al.* [1995]. Hydroperoxides were separated by reverse phase HPLC on a 5μ Inertsil ODS-2 PEEK column (4.6 mm × 250 mm, Alltech) followed by a postcolumn derivatization reaction forming a fluorescent dimmer. The peroxidase catalyzed dimerization of p-hydroxyphenyl acetic acid occurs in the presence of peroxy functional groups at elevated pH. Formation of the fluorescent dimmer is proportional to the concentration of a given hydroperoxide [*Kok et al.*, 1995; *Lee et al.*, 1995]. The detection limits for H_2O_2 and CH_3OOH were 15 and 25 pptv, respectively, for the TRP program (3 times the standard deviation of the blank). The estimated accuracy for each measurement is 15% for H_2O_2 and 25% for CH_3OOH and includes the uncertainties in aqueous peroxide standards, blanks, gas flow rates, aqueous flow rates and collection efficiency for CH_3OOH. Details regarding the system configurations for the PWA, and PWB and PTA programs are given by *Heikes et al.* [1996] and *O'Sullivan et al.* [1999], respectively.

[8] For the PTB field campaign the HPLC injection process was automated. In the previous Pacific exploratory missions the collection solutions from the stripping coils were collected in 5-ml PFA Teflon vials and injected by hand at 2.5- or 5-min intervals for the DC-8 and P3-B, respectively. This configuration resulted in an individual injection representing an "integrated sample" over the collection interval, 2.5 or 5 min. During PTB and the TRP program, the collection solutions from the coils were pumped continuously through the HPLC injection valve loop. Every 2.5 or 5 min, the valve was actuated and an injection performed (Valco Instruments, Inc.). Consequently, the peroxide injection represents a 30-s snapshot of atmospheric peroxide levels which were observed on a 2.5- or 5-min cycle.

[9] SO_2 was measured by atmospheric pressure ionization mass spectrometry during TRP with a detection limit of <1 pptv at the 2σ level when the measurements were averaged to 1 s [*Thornton et al.*, 2002]. CO_2 was measured with Li Cor® 6252 nondispersive infrared analyzers during TRP; the 1-s averaged data have a 1σ precision of 0.070 ppmv with an accuracy of ±0.2 ppmv [*Vay et al.*, 2003]. Methane and CO were measured with tunable diode laser systems [*Sachse et al.*, 1987, 1991] with accuracies of ±1% for CH_4 and ±2% for CO compared to NOAA/CMDL standards for the TRP program [*Bartlett et al.*, 2003]. Analytical protocals for the measurement of the nonmethane hydrocarbons and halocarbons are given by *Blake et al.*

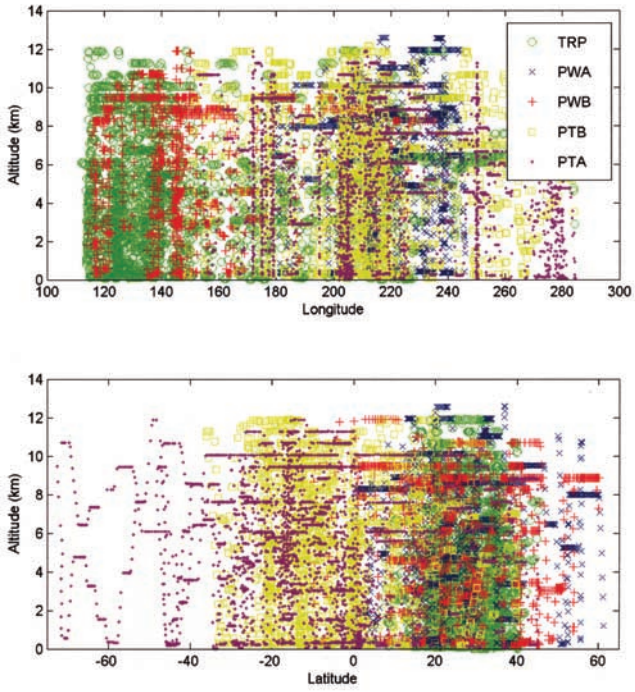

Figure 2. Sample locations for the various GTE field programs.

[1996, 2003, and references there in]. O_3 was determined by chemiluminescence with an accuracy of 3% or 2 ppbv [*Hoell et al.*, 1997], and NO was determined by LIF with an accuracy of ±18% [*Bradshaw et al.*, 1999]. Gas phase HNO_3 measurements for TRP are described by *Talbot et al.* [2003] and have a precision and accuracy of 10–20%. Analytical figures of merit for earlier missions are available with the mission data from the NASA-Langley Distributed Active Archive Center or via the GTE homepage (http://www-gte.larc.nasa.gov).

3. Results

[10] The geographic and vertical locations of the samples are shown in Figure 2 for each field program. From these plots it is evident that the data coverage within each region is not equivalent; latitudes greater than 45° are not well sampled during the GTE missions. Hence some regional averages are based on observations from only a few flights in a particular field program. The regional averages, standard deviations, and number of observations for each field program and for each chemical species are presented in Table 2. Each field programs regional average mixing ratio for a species is the average from all observations at all altitudes within the region. Differences in the frequency of observations at various altitudes between field programs could have a significant effect on the regional averages. For species that exhibit small gradients with altitude the effect would be minimal; however, for species with substantial vertical gradients, such as H_2O_2, the impact of a difference in the number of samples at a given altitude could be significant. To determine if the number of samples at a given altitude in a region was similar between programs, the cumulative distribution functions of altitude for samples in a given region between programs were compared; see Figure 3 (HLNP is not shown). The closest correspondence between missions with respect to vertical sample distributions in a given region is generally between the paired GTE missions, for example, PWA and PWB and PTA and PTB. In the MNEP the coverage with altitude between missions is quite similar (with the exception of PWB) up to 7–8 km where some divergence is observed. During PWB the MNEP observations are dominated by altitudes >7 km. In the MNWP the distribution with altitude between missions is quite similar with the exception of a greater number of observations in the 1- to 2-km altitude range during TRP (Figure 3). Generally, H_2O_2 will exhibit a maximum around this altitude range, and one would expect a larger regional average mixing ratio for TRP. In fact, the opposite is observed, and this is discussed in section 3.3. Depending on the objectives of a particular field campaign, some regions were not sampled at all during a particular program. For the discussions that follow we focus on species for which there are observations spanning at least three field programs. A few regions like the MNEP have observations from all GTE missions, although the number of observations comprising the regional mission average for a species varies. The HLSP region has the fewest observations, the paucity of data for this region does not permit the analysis of long-term changes. If sufficient data existed within a region, changes in the altitude distribution of species over time were examined.

[11] Of the five field missions, PWA and PTA and PWB, PTB, and TRP exhibit the greatest overlap in species distribution patterns and concentrations [*O'Sullivan et al.*, 1999]. The greatest differences arise when viewing the "A" missions relative to the "B" missions and TRP. Both the "A" campaigns occurred in the fall, nominally, September to October, and the "B" missions and TRP occurred in the spring, generally late February to April (Table 1). PWB and TRP offer the best scenario for examining long-term changes in pollutant loading over the Pacific since these missions occurred at similar times during the year (offset by 3 weeks and have the greatest correspondence between flight tracks and hence data coverage. In addition, these programs sampled the Pacific troposphere when the multivariate ENSO index ranking indicates near normal El Niño conditions [*Fuelberg et al.*, 2003]. PWB and TRP are compared in section 3.3.

3.1. Peroxides and O_3

[12] Over the last 15 years, there have been a number of measurements of peroxides in the troposphere. A variety of different analytical methods and field results through 1990 have been reviewed by *Gunz and Hoffmann* [1990] and *Sakugawa et al.* [1990]. Observations since 1990 including an expanding number of organic peroxide measurements have been reviewed by *Lee et al.* [2000]. The ground- and aircraft-based programs have demonstrated that H_2O_2 is the dominant peroxide present in the troposphere. The most abundant organic peroxide is CH_3OOH or hydroxymethylhydroperoxide (HMHP) ($HOCH_2OOH$) [*Hewitt and Kok*, 1991; *Heikes*, 1992; *Heikes et al.*, 1996; *Lee et al.*, 1993; *Ayers et al.*, 1996; *Fels and Junkermann*, 1994; *Tremmel e al.*, 1993, 1994; *McDonald et al.*, 1995; *Watkins et al.*, 1995a, 1995b; *Weinstein-Lloyd et al.*, 1996, 1998;

Table 2. Regional Mean Concentrations of Selected Chemical Species for the GTE Mission Over the Pacific Ocean[a]

	H_2O_2, pptv					CH_3O_2H, pptv					SO_2, pptv					CO_2, ppm				
	PWA	PWB	PTA	PTB	TRP	PWA	PWB	PTA	PTB	TRP	PWA	PWB	PTA	PTB	TRP	PWA	PWB	PTA	PTB	TRP
										HLNP										
Mean	397	152	925	-	167	315	84	465	-	104	133	96.1	21.6	-	31	-	360.8	365.8	-	375.3
SD	347	85	418	-	5	230	73	177	-	10	130	123	10.7	-	7	-	2.5	0.84	-	0.4
Number	210	141	9	-	3	210	120	9	-	3	210	141	9	-	3	-	141	9	-	3
										MNEP										
Mean	614	398	759	862	671	535	154	505	371	421	74.5	35.5	21.9	54.5	79	352.7	359.6	359.8	369.1	372.8
SD	414	373	530	755	524	367	103	350	269	310	47.2	8.9	44.3	67.6	189	0.63	1.5	1.5	1.3	1.5
Number	265	79	434	489	310	225	78	409	424	245	172	26	296	361	548	222	79	416	542	847
										MNWP										
Mean	924	670	-	-	614	600	237	-	-	266	117	124[b]	-	-	443[c]	352.3	359.8	-	-	374.0
SD	649	1011	-	-	732	483	267	-	-	255	138	303	-	-	1269	1.1	2.39	-	-	2.84
Number	1125	1157	-	-	1003	1075	1063	-	-	736	809	859	-	-	1661	1189	1124	-	-	2595
										EQEP										
Mean	-	-	1351	1242	-	-	-	677	822	-	-	-	42.6	53.0	-	-	-	361.3	368.2	-
SD	-	-	1024	814	-	-	-	409	598	-	-	-	30.6	145.7	-	-	-	0.60	0.90	-
Number	-	-	689	790	-	-	-	641	480	-	-	-	565	581	-	-	-	687	720	-
										EQWP										
Mean	1097	811	667	731	-	957	578	716	1044	-	58.7	31.8	25.6	25.5	66.8	353.3	358.5	361.0	368.0	371.5
SD	1023	778	452	426	-	659	404	484	388	-	33.5	49.0	25.1	15.6	42.6	0.2	0.7	0.4	0.8	0.7
Number	169	222	78	26	-	169	228	76	26	-	166	164	68	26	29	177	196	77	26	29
										MSEP										
Mean	-	-	669	894	-	-	-	429	641	-	-	-	23.6	42.1	-	-	-	361.0	366.5	-
SD	-	-	585	778	-	-	-	344	462	-	-	-	26.2	33.5	-	-	-	0.5	0.9	-
Number	-	-	1572	1149	-	-	-	1389	978	-	-	-	1215	1115	-	-	-	1578	1226	-
										MSWP										
Mean	-	378	704	430	-	-	487	426	408	-	-	63.7	34.6	30.8	-	-	357.4	361.0	366.3	-
SD	-	307	605	317	-	-	298	386	482	-	-	51.9	227	16.5	-	-	0.4	0.5	0.8	-
Number	-	36	395	236	-	-	38	435	184	-	-	29	395	251	-	-	29	348	271	
										HLSP										
Mean	-	-	280	-	-	-	-	302	-	-	-	-	8.5	-	-	-	-	360.6	-	-
SD	-	-	280	-	-	-	-	251	-	-	-	-	7.8	-	-	-	-	0.4	-	-
Number	-	-	214	-	-	-	-	196	-	-	-	-	169	-	-	-	-	197	-	-

	CO, ppb					O_3, ppb					CH_4, ppb					NO, pptv				
	PWA	PWB	PTA	PTB	TRP	PWA	PWB	PTA	PTB	TRP	PWA	PWB	PTA	PTB	TRP	PWA	PWB	PTA	PTB	TRP
										HLNP										
Mean	91.4	139.0	98.3	-	151.7	73.7	83.0	48.0	-	68.3	1749	1762	-	-	1815	11.2	11.7	10.2	-	15.0
SD	18.8	44.3	15.6	-	9.0	73.8	74.4	17.7	-	1.9	47	47	-	-	4.1	14.2	9.96	6.3	-	1.5
Number	210	141	9	-	3	210	141	9	-	3	210	141	-	-	3	210	141	9	-	3
										MNEP										
Mean	80.7	131.3	68.6	100.8	113	35.2	57.3	36.9	42.3	60.9	1722	1749	1733	1761	1774	16.5	27.7	14.6	11.0	26.0
SD	15.1	41.0	18.4	28.4	62	15.6	19.2	21.8	16.0	59.5	17	27	22	15	30	27.3	21.2	23.5	9.1	49.5
Number	280	76	429	542	857	317	79	358	490	823	280	66	270	215	677	271	77	120	402	692
										MNWP										
Mean	98.5	132.1	-	-	160.8	37.4	51.8	-	-	56.3	1738	1752	-	-	1796	27.0	39.6	-	-	43.2
SD	22.7	62.3	-	-	87.2	20.6	41.8	-	-	27.8	33	42	-	-	38	59.8	51.6	-	-	139
Number	1417	1107	-	-	2623	1480	1172	-	-	2674	1421	949	-	-	2310	1286	1143	-	-	2222
										EQEP										
Mean	-	-	74.4	67.7	-	-	-	29.3	17.0	-	-	-	1714	1739	-	-	-	17.0	8.3	-
SD	-	-	37.8	12.2	-	-	-	16.0	9.9	-	-	-	13	19	-	-	-	17.3	9.4	-
Number	-	-	689	715	-	-	-	715	839	-	-	-	620	242	-	-	-	462	755	-
										EQWP										
Mean	81.0	93.7	56.3	64.1	95.9	18.5	26.4	19.9	12.5	32.0	1686	1726	1708	1737	1764	10.2	21.5	11.6	3.76	11.0
SD	16.5	24.6	3.3	9.5	17.8	7.6	11.5	8.0	4.3	11.6	10	12	10	14	10	8.2	31.2	15.2	2.7	2.9
Number	202	219	78	24	29	206	229	79	26	29	202	181	78	26	26	199	216	63	9	29
										MSEP										
Mean	-	-	65.6	48.6	-	-	-	48.7	22.7	-	-	-	1704	1714	-	-	-	26.0	14.8	-
SD	-	-	19.7	7.6	-	-	-	25.9	10.7	-	-	-	12	14	-	-	-	33.0	29.1	-
Number	-	-	1578	1218	-	-	-	1617	1297	-	-	-	1467	769	-	-	-	703	1000	-

Table 2. (continued)

	CO, ppb					O_3, ppb					CH_4, ppb					NO, pptv				
	PWA	PWB	PTA	PTB	TRP	PWA	PWB	PTA	PTB	TRP	PWA	PWB	PTA	PTB	TRP	PWA	PWB	PTA	PTB	TRP
MSWP																				
Mean	-	61.9	71.4	48.4	-	-	20.6	46.4	19.1	-	-	1682	1707	1714	-	-	44.6	27.6	14.2	-
SD	-	7.9	15.0	6.0	-	-	10.1	22.2	9.6	-	-	13	11	11	-	-	44.1	35.7	14.6	-
Number	-	29	487	246	-	-	39	478	279	-	-	19	430	232	-	-	39	366	189	-
HLSP																				
Mean	-	-	67.9	-	-	-	-	56.8	-	-	-	-	1693	-	-	-	-	5.63	-	-
SD	-	-	18.5	-	-	-	-	46.7	-	-	-	-	11	-	-	-	-	8.1	-	-
Number	-	-	207	-	-	-	-	228	-	-	-	-	222	-	-	-	-	166	-	-

	HNO_3, pptv					PAN, pptv					DMS, pptv					C_2H_6, pptv				
	PWA	PWB	PTA	PTB	TRP	PWA	PWB	PTA	PTB	TRP	PWA	PWB	PTA	PTB	TRP	PWA	PWB	PTA	PTB	TRP
HLNP																				
Mean	80.2	288	69.5	-	78	95	209	96	-	302	72	11.3	-	-	-	-	1643	685	-	1711
SD	91.4	389	57.6	-	15	65	156	75	-	46	78	6.3	-	-	-	-	735	73	-	140
Number	210	141	9	-	3	210	141	9	-	2	210	141	-	-	-	-	141	9	-	3
MNEP																				
Mean	57.9	178.8	77.8	74.3	151	19.0	145	49	66	100	10.5	2.2	49.1	8.0	4.9	-	1154	420	897	951
SD	70.1	45.1	93.6	69.1	195	19.5	141	52	50	97	9.2	-	93.3	6.5	6.5	-	551	142	401	393
Number	160	53	338	506	538	170	58	182	257	732	98	1	103	41	155	-	73	325	501	784
MNWP																				
Mean	76.2	258	-	-	274	50.5	221	-	-	280	22.2	7.91	-	-	6.3	622	1129	-	-	1342
SD	90.3	467	-	-	344	61.3	260	-	-	334	24.1	6.5	-	-	6.2	254	712	-	-	707
Number	858	954	-	-	1989	828	756	-	-	2270	411	181	-	-	525	155	956	-	-	2542
EQEP																				
Mean	-	-	68.0	44.4	-	-	-	21	38	-	-	-	43.0	73.5	-	-	-	472	455	-
SD	-	-	70.0	41.7	-	-	-	28	43	-	-	-	32.5	57.5	-	-	-	308	192	-
Number	-	-	461	788	-	-	-	186	192	-	-	-	331	302	-	-	-	579	720	-
EQWP																				
Mean	22.8	169	41.3	26.8	73.0	9.8	22	7.3	8.0	29	13.9	7.6	64.4	ND	11.3	426	608	259	419	609
SD	17.3	137	21.2	11.3	26.0	7.9	23	6.3	5.4	19	16.5	7.4	52.2	ND	10.5	149	129	31	109	117
Number	89	156	77	26	21	143	106	56	13	23	92	118	41	ND	12	43	206	76	26	29
MSEP																				
Mean	-	-	90.2	46.4	-	-	-	64	21	-	-	-	25.5	84.3	-	-	-	391	253	-
SD	-	-	112	33.3	-	-	-	88	16	-	-	-	38.0	101	-	-	-	167	75	-
Number	-	-	1352	1144	-	-	-	821	624	-	-	-	268	199	-	-	-	1343	1168	-
MSWP																				
Mean	-	180.1	101.5	42.7	-	-	20.1	57.6	25	-	-	24.4	22.0	-	-	-	315	385	244	-
SD	-	49.6	87	39.4	-	-	18.8	60.2	31	-	-	25.3	28.8	-	-	-	112	131	64	-
Number	-	37	436	245	-	-	27	337	196	-	-	21	133	-	-	-	35	378	237	-
HLSP																				
Mean	-	-	153.8	-	-	-	-	45	-	-	-	-	11.8	-	-	-	-	373	-	-
SD	-	-	253	-	-	-	-	55	-	-	-	-	13.4	-	-	-	-	126	-	-
Number	-	-	179	-	-	-	-	160	-	-	-	-	149	-	-	-	-	196	-	-

	C_3H_8, pptv					C_2H_2, pptv					C_2Cl_4, pptv					CH_3I, pptv				
	PWA	PWB	PTA	PTB	TRP	PWA	PWB	PTA	PTB	TRP	PWA	PWB	PTA	PTB	TRP	PWA	PWB	PTA	PTB	TRP
HLNP																				
Mean	-	583	84	-	458	-	470	140	-	418	4.57	14.0	4.64	-	10.6	-	0.13	0.22	-	0.08
SD	-	389	27	-	76	-	271	79	-	55	2.40	7.6	0.6	-	0.6	-	0.10	0.24	-	0.015
Number	-	141	9	-	3	-	141	9	-	3	210	141	9	-	3	-	141	9	-	3
MNEP																				
Mean	-	257	31	120	148	-	318	46	166	227	4.46	9.25	2.64	4.12	4.46	-	0.14	0.19	0.21	0.18
SD	-	247	24	139	134	-	247	45	121	142	6.68	4.25	1.29	2.11	2.46	-	0.11	0.21	0.18	0.20
Number	-	73	325	501	761	-	73	325	501	759	192	73	325	498	755	-	69	325	499	684
MNWP																				
Mean	80	282	-	-	326	83	333	-	-	430	4.66	10.1	-	-	7.09	-	0.18	-	-	0.27
SD	99	341	-	-	340	111	354	-	-	427	5.73	7.1	-	-	9.22	-	0.22	-	-	0.25
Number	155	956	-	-	2532	122	954	-	-	2542	122	921	-	-	2540	-	942	-	-	2543
EQEP																				
Mean	-	-	36.1	26.3	-	-	-	69	38	-	-	-	1.43	2.31	-	-	-	0.24	0.23	-

Table 2. (continued)

	C_3H_8, pptv					C_2H_2, pptv					C_2Cl_4, pptv					CH_3I, pptv				
	PWA	PWB	PTA	PTB	TRP	PWA	PWB	PTA	PTB	TRP	PWA	PWB	PTA	PTB	TRP	PWA	PWB	PTA	PTB	TRP
SD	-	-	37	48.6	-	-	-	108	23	-	-	-	0.24	0.71	-	-	-	0.19	0.17	-
Number	-	-	579	717	-	-	-	579	719	-	-	-	580	719	-	-	-	580	715	-
										EQWP										
Mean	35.2	51	15	16	41	33	95	23	32	132	1.92	6.00	1.45	2.27	3.00	-	0.24	0.20	0.26	0.30
SD	26	18	4	8	19	33	83	10	13	62	0.68	1.07	0.26	0.65	0.81	-	0.22	0.11	0.12	0.24
Number	37	206	69	26	29	37	206	69	26	29	99	196	57	26	29	-	201	69	26	29
										MSEP										
Mean	-	-	27	7.8	-	-	-	62	16	-	-	-	1.39	1.26	-	-	-	0.12	0.18	-
SD	-	-	22	4.7	-	-	-	49	8	-	-	-	0.32	0.31	-	-	-	0.15	0.18	-
Number	-	-	1335	1052	-	-	-	1343	1167	-	-	-	1296	1150	-	-	-	1347	1169	-
										MSWP										
Mean	-	28	25	6.00	-	-	21.9	70.4	15.6	-	-	3.69	1.30	1.27	-	-	0.18	0.13	0.19	-
SD	-	14	12	2.9	-	-	11	40.0	6.7	-	-	0.85	0.26	0.34	-	-	0.12	0.13	0.12	-
Number	-	34	378	197	-	-	35	378	237	-	-	35	361	237	-	-	35	378	236	-
										HLSP										
Mean	-	-	33	-	-	-	-	71.3	-	-	-	-	1.17	-	-	-	-	0.10	-	-
SD	-	-	14	-	-	-	-	34.8	-	-	-	-	0.54	-	-	-	-	0.08	-	-
Number	-	-	196	-	-	-	-	196	-	-	-	-	182	-	-	-	-	196	-	-

[a]SD is standard deviation.
[b]Data impacted by SO_2 emissions from volcanoes were removed to compute the regional average; all these values were >10 ppbv.
[c]During the TRP program flights 16 and 17 on the P-3B flew through emissions from Miyake-Jima volcano; data from these flight legs were excluded from the regional average.

O'Sullivan et al., 1999]. CH_3OOH is the dominant organic peroxide in the remote marine troposphere; HMHP is more prevalent over continental regions. The majority of investigations have focused on the northeastern United States, and only a few have sampled in multiple seasons [*Olszyna et al.*, 1988; *Claiborn and Aneja*, 1991; *Ayers et al.*, 1992; *McDonald et al.*, 1995] or over several years. A seasonal decrease of nearly a factor of 5 in H_2O_2 mixing ratios has been observed for the continental northeastern United States and reflects the seasonal transition from a NO_x-limited to a hydrocarbon-limited photochemical regime [*Jacob et al.*, 1995]. *Ayers et al.* [1992] observed seasonal variations in peroxides in the marine troposphere from a site at Cape Grim. The seasonal cycle in the concentration of peroxides had an amplitude of about 1.5 ppbv, with a minimum in June–July (Southern Hemisphere winter) and a maximum in December–January in the lower troposphere at Cape Grim.

[13] Since the PWA and PTA field programs occurred at the same time of year nominally September to October and PWB, PTB, and TRP occurred from February to April, the differences in the mean mixing ratios of these species in part reflect seasonally driven changes. For the discussion that follows, the September to October missions (PWA and PTA) will be considered fall and the February to April missions (PWB, PTB, and TRP) spring, since the bulk of the flight observations are in the Northern Hemisphere. By examining the mission mean mixing ratios for a particular compound, it is apparent that all species exhibit a seasonal signal to some extent, Table 2. For some species the signal maybe driven largely by seasonal photochemical changes, source emission shifts, and/or transport changes. The sampling frequency with respect to altitude and location was not evenly distributed throughout the five different field campaigns (Figure 2). Consequently, the mean mixing ratio for a particular region is composed of a unique number of observations. In the mid-latitudes and tropics the five missions have produced a robust data set at all altitudes; however, at high latitudes, particularly in the extreme Northern and Southern Hemispheres, the data coverage is sparse. Caution should be exercised when comparing regional averages between programs when the sampling rate for the region is vastly different.

[14] If one compares the regional averages between the paired PWA and PWB programs and the PTA and PTB programs, it is reasonable to expect long-term process influencing the peroxide distributions will be somewhat muted. Hence the differences will largely be due to seasonal effects. During the PEM West programs the mean mixing ratios of H_2O_2 and CH_3OOH were higher during the PWA campaign in all the regions (Table 2). H_2O_2 mixing ratios were 38 ± 16% higher [Δ(fall-spring) 258 ± 34 pptv], and CH_3OOH was 61 ± 15% higher (Δ343 ± 76 pptv) through out the Pacific troposphere. These variations are well within the anticipated seasonal variations as a result of photochemical regime changes. However, a similar comparison of the paired PTA and PTB missions does not produce a consistent pattern for the regional averages. During these missions only the EQEP and MSWP regions exhibit higher mixing ratios during the fall. *Olson et al.* [2001] examined the altitude distributions for H_2O_2 and CH_3OOH during PTA and PTB and found that PTA exhibited the largest median values in all but one altitude bin, with the greatest differences between missions occurring below 2 km. The observed differences were qualitatively consistent with the calculated seasonal HO_2 distributions from a photochemical box model.

[15] Mixing ratios for H_2O_2 and CH_3OOH exhibit the largest seasonal differences (fall-spring) in the MNEP region, ΔH_2O_2 = 375 pptv and ΔCH_3OOH = 397 pptv (Table 2). Seasonal differences in the other regions are also quite evident. No data are available for the high-latitude south Pacific during the spring; the fall data in

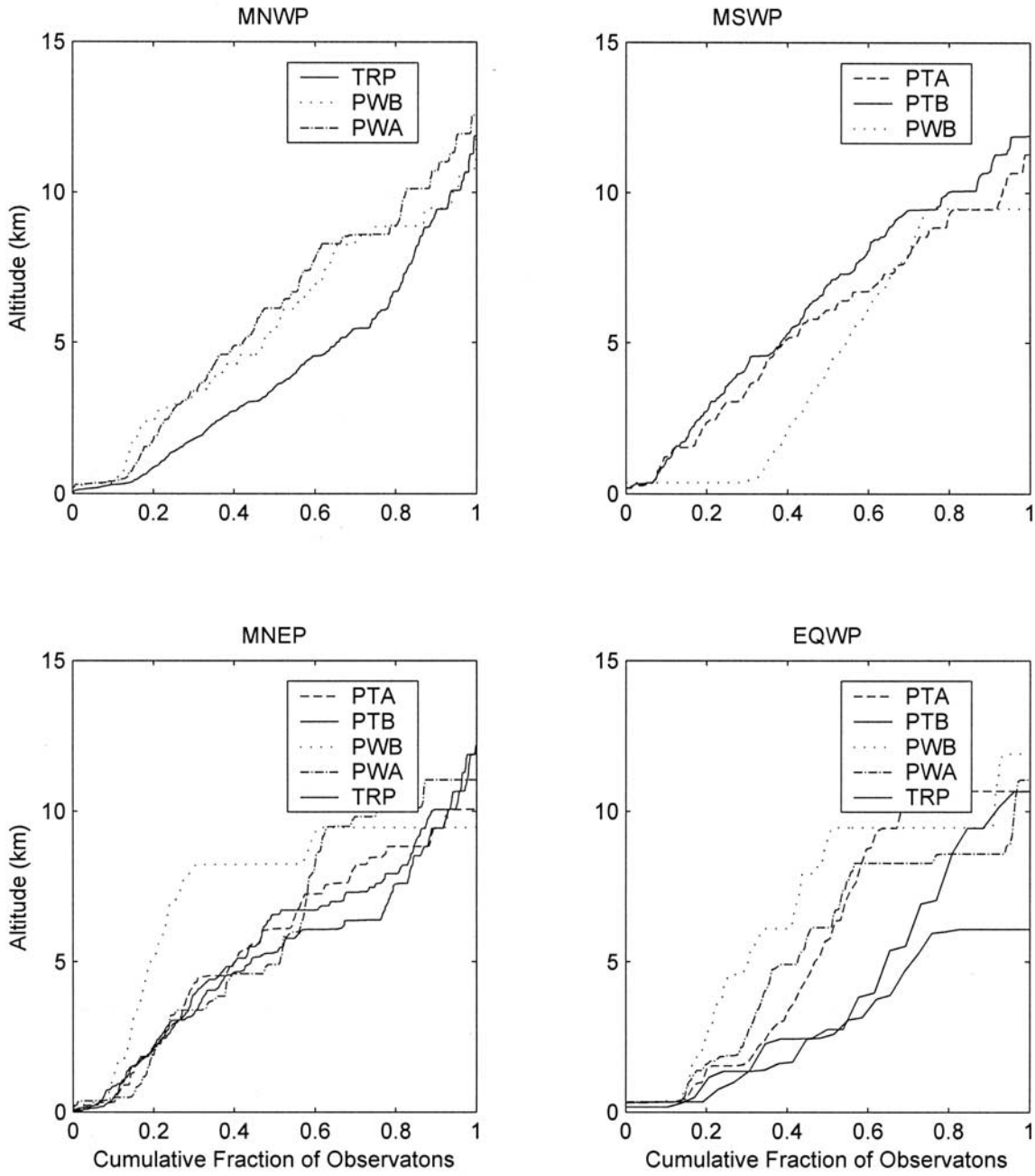

Figure 3. The cumulative distribution function with altitude for samples composing the regional average species mixing ratios for the GTE missions with data for the particular region.

this region are made up of one flight during PEM Tropics A. The relative change on a seasonal basis shows a maximum for H_2O_2 in the HLNP with a 95% change in the average mixing ratio between the fall and spring season followed by MNEP and MSEP at around 50%. The smallest seasonal changes occur for the EQEP, EQWP, and MNWP regions, 8, 18, and 14%, respectively, for H_2O_2. Methylhydroperoxide behaves quite differently. The largest seasonal changes are observed in the HLNP and MNEP regions with changes of 118% and 95%, respectively. The remaining regions exhibit a 20–40% seasonal change in CH_3OOH mixing ratios with the exception of the MSEP region, which exhibits no seasonal signal. The seasonal changes from fall to spring are only a fraction of the changes anticipated for the peroxides if the maximum and minimum seasons had been sampled. For example, *Ayers et al.* [1992] observed the seasonal cycle in H_2O_2 mixing ratio at 100 m altitude on the seaward edge of Cape Grim at 41°S. Their observations indicated a maximum seasonal change of nearly an order of magnitude from June–July to November–December, minimum and maximum in the Southern Hemisphere, respectively. *Ayers et al.* [1992] observations for spring and fall differ by 10–15%, which is similar to the change observed in this work for that region. Unfortunately, the NASA GTE field campaigns did not sample during the summer and winter seasons, which would have afforded the

opportunity to sample the maximum and minimum peroxide mixing ratios.

[16] A seasonal cycle in peroxide concentrations is anticipated based on seasonally driven changes in photochemical production and loss mechanisms. However, changes in vertical and horizontal transport regimes during different seasons also have a dramatic influence on the observed distributions of the peroxides. The meteorological settings for the fall missions were described by *Bachmeier and Fuelberg* [1996] for PWA and *Fuelberg et al.* [1999] for PTA. Meteorological settings for the spring missions were described by *Merrill et al.* [1997] for PWB and *Fuelberg et al.* [2001] for PTB. Meteorological process leading to enhanced continental outflow are more prevalent in the spring. The impact of continental sources on the distribution of the peroxides is evident in Figures 4 and 5. At the lowest altitudes, 0–2 km and 2–4 km, elevated peroxides are observed near coastal sources in both the western and eastern Pacific. The influence of the proximity of the Asian coast is most evident in the spring, particularly for H_2O_2 [*O'Sullivan et al.*, 1999]. The highest H_2O_2 mixing ratios were observed in recent pollution plumes originating over Asia during the spring [*Heikes et al.*, 1996]. Similar trends are observed for CO and C_2Cl_4 supporting the influence of pollution plumes on the peroxide distributions. C_2Cl_4 also exhibits a strong source signature southeast of Japan (not shown). Further support of the importance of recent emission is gleaned from the ratio of ethyne to CO (Figure 6). *Smyth et al.* [1996] developed the ratio of ethyne to CO as a measure of air mass processing. Processing of the air mass occurs via two mechanisms, photochemical oxidation by hydroxyl or by mixing continentally influence air masses with photochemically processed air. This ratio is a proxy for the age of the air mass; higher ratios indicate recent exposure to surface emissions. The C_2H_2/CO ratios clearly indicate the influence of recent outflow in spring in the western Pacific at all altitudes. The occurrence of outflow appears to be substantially reduced in the fall in this region (Figure 6).

[17] In the eastern Pacific the peroxides are influenced by outflow from coastal South America extending into the eastern Pacific troposphere. At the surface the flow is predominantly from the southeast originating in the subtropical anticyclone near 30°S [*Fuelberg et al.*, 1999]. The surface peroxide levels are likely influenced by coastal, low-altitude sources. At 2–4 km the winds are easterly (offshore) north of 10°S and have trajectories that have passed over interior regions of South America. The highest mixing ratios for the peroxides were observed at 2–4 km in this region, CO also exhibits elevated levels. C_2Cl_4 is not elevated suggesting that the principal pollution source is not industrial. Biomass burning is prevalent in South America and its influence extends into the eastern Pacific troposphere [*Talbot et al.*, 1999; J. A. Logan et al., Analysis of biomass burning plumes in the tropical Pacific during PEM Tropics, unpublished manuscript, 2003].

[18] In both the spring and fall elevated concentrations of H_2O_2 and CH_3OOH were observed off the coast of California in the 4- to 8-km altitude range (Figures 4 and 5). At this altitude the mean streamlines are westerly in the spring [*Fuelberg et al.*, 2001], cyclonic activity in Asia uplifts air which is transported east and descends off the coast of California. The ratio of C_2H_2/CO is elevated supporting a rapid transport scenario. *Clark et al.* [2001] examined the origin of aerosols and pollutants in the air mass and have shown that 10-day back trajectories of the air mass touch down in the vicinity of Japan and the southern Gobi desert. Elevated levels of CH_3OOH are evident at high altitude in the spring northeast of the South Pacific Convergence Zone (SPCZ). The SPCZ is more defined in the spring than in the fall, which is evident in the absence of elevated CH_3OOH at altitude near the SPCZ in the fall (Figure 5). During the fall both peroxides are transported to altitudes greater than 8 km by the Intertropical Convergence Zone (ITCZ) in the central Pacific (Figures 4 and 5). At higher altitudes, deep convection has been suggested as the cause of the difference between observed and modeled peroxide concentrations [*Prather and Jacob*, 1997; *Cohan et al.*, 1999]. These data clearly show this phenomenon and demonstrate the importance of the SPCZ and ITCZ in influencing the distributions of peroxides with altitude in these regions. Previous work has demonstrated the importance of these convergence zones as a barrier for exchange at altitudes below 5 km [*Gregory et al.*, 1999]. These data indicate the importance the convergence zones play in the vertical distribution of species and the resulting change in photochemical processes.

[19] The levels of O_3 in the troposphere are influenced by in situ photochemistry and transport processes. At altitudes >8 km in the high-latitude north and south the DC-8 sampled stratospheric air as a result of intrusions and sampled the lower altitude of the tropopause at high latitudes [*Browell et al.*, 1996] (Figure 7) (high-latitude Southern Hemisphere is not shown). At altitudes below 2 km, net destruction of O_3 in the marine boundary layer is evident by the low mixing ratio observed through out the tropical and south Pacific regions; at higher altitudes the O_3 mixing ratio increases (Figures 8 and 9). The O_3 mixing ratio in the MSEP and MSWP are a factor of 2 higher during the fall (Table 2). *Wu et al.* [1997] observed a greater frequency of encounters with high O_3 layers in the Pacific troposphere during the fall. The most prevalent type of layer contained high O_3 and low water vapor and was associated with midlatitude stratospheric subsidence reaching into the tropics. In the spring the number of layers associated with polluted continental air was only one third of the number observed during the fall. The presences and absence of these layers clearly influences regional, seasonal changes in O_3 mixing ratios in the Pacific troposphere.

3.2. Long-Lived Species: CH_4 and CO_2

[20] Both CH_4 and CO_2 are long-lived species in the atmosphere and contribute to the greenhouse effect. Methane is an important trace component of the atmosphere, impacting both tropospheric and stratospheric chemical cycles [*Cicerone and Oremland*, 1988]. The primary removal process for tropospheric methane is reaction with hydroxyl radical, resulting in an atmospheric methane lifetime of about 8 years. In the troposphere large fluxes of methane could suppress hydroxyl radical levels impacting the ozone and HO_x budgets, altering the oxidative capacity of the atmosphere. Methane is also about 20 times more effective on a weight basis than carbon dioxide as a greenhouse gas and currently accounts for about 15% of enhanced greenhouse forcing [*Lashof and Ahuja*, 1990]. The annual atmospheric

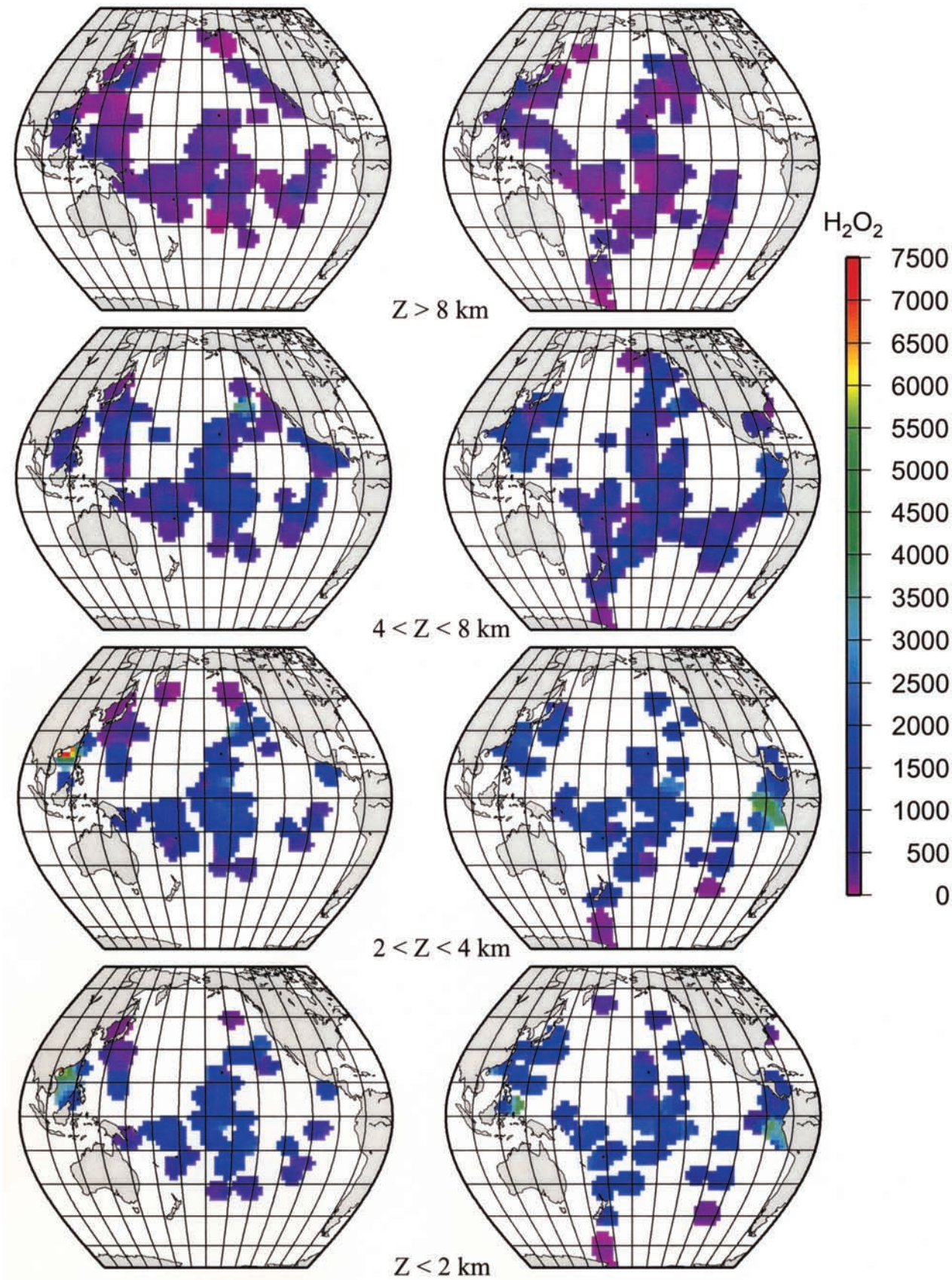

Figure 4. The distribution of hydrogen peroxide in the troposphere over the Pacific during the (left) spring (PWB and PTB) and (right) fall (PWA and PTA) as a function of altitude. The concentrations are in parts per trillion by volume.

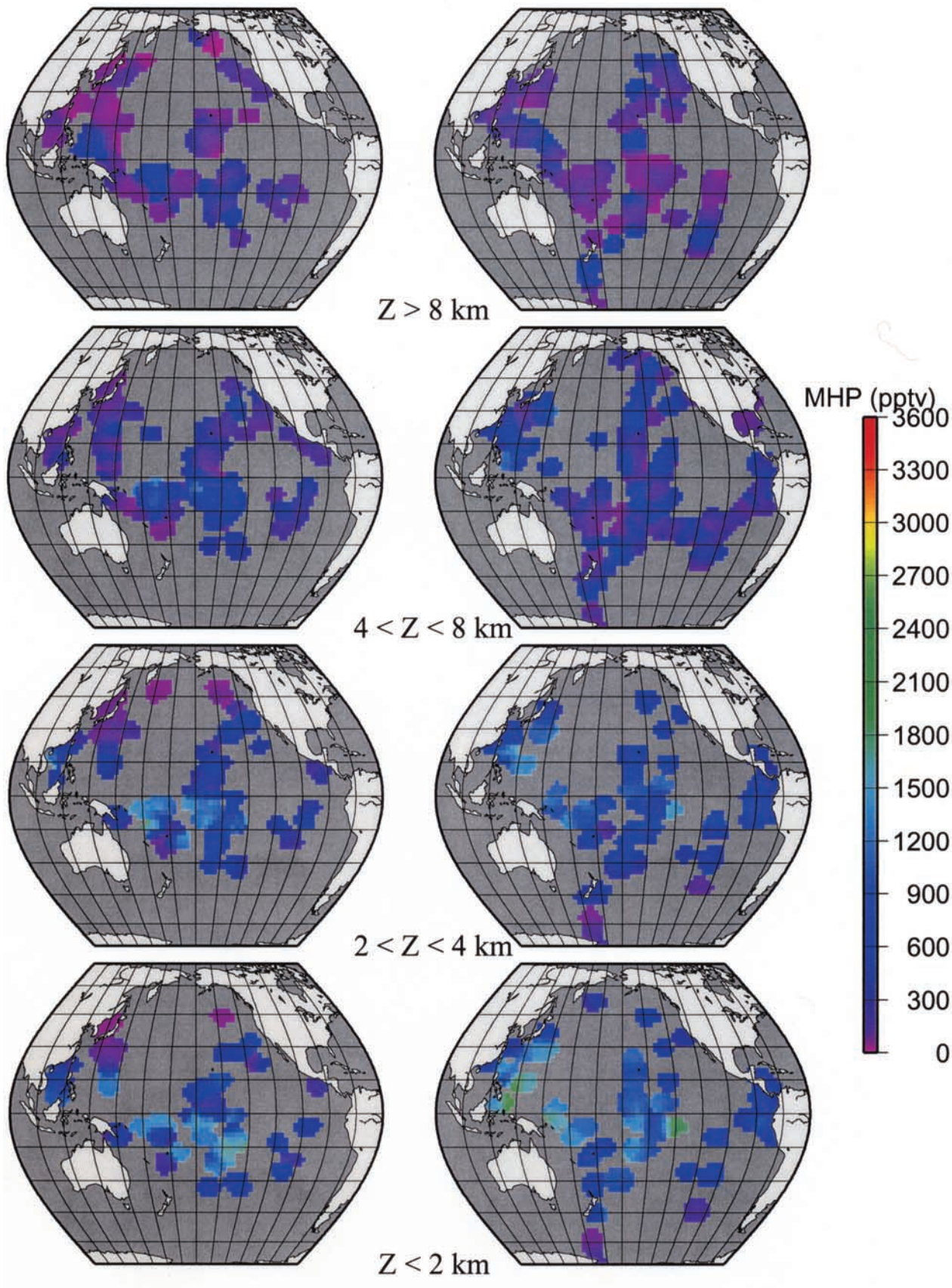

Figure 5. The distribution of methylhydroperoxide in the troposphere over the Pacific during the (left) spring (PWB and PTB) and (right) fall (PWA and PTA) as a function of altitude. The concentrations are in parts per trillion by volume.

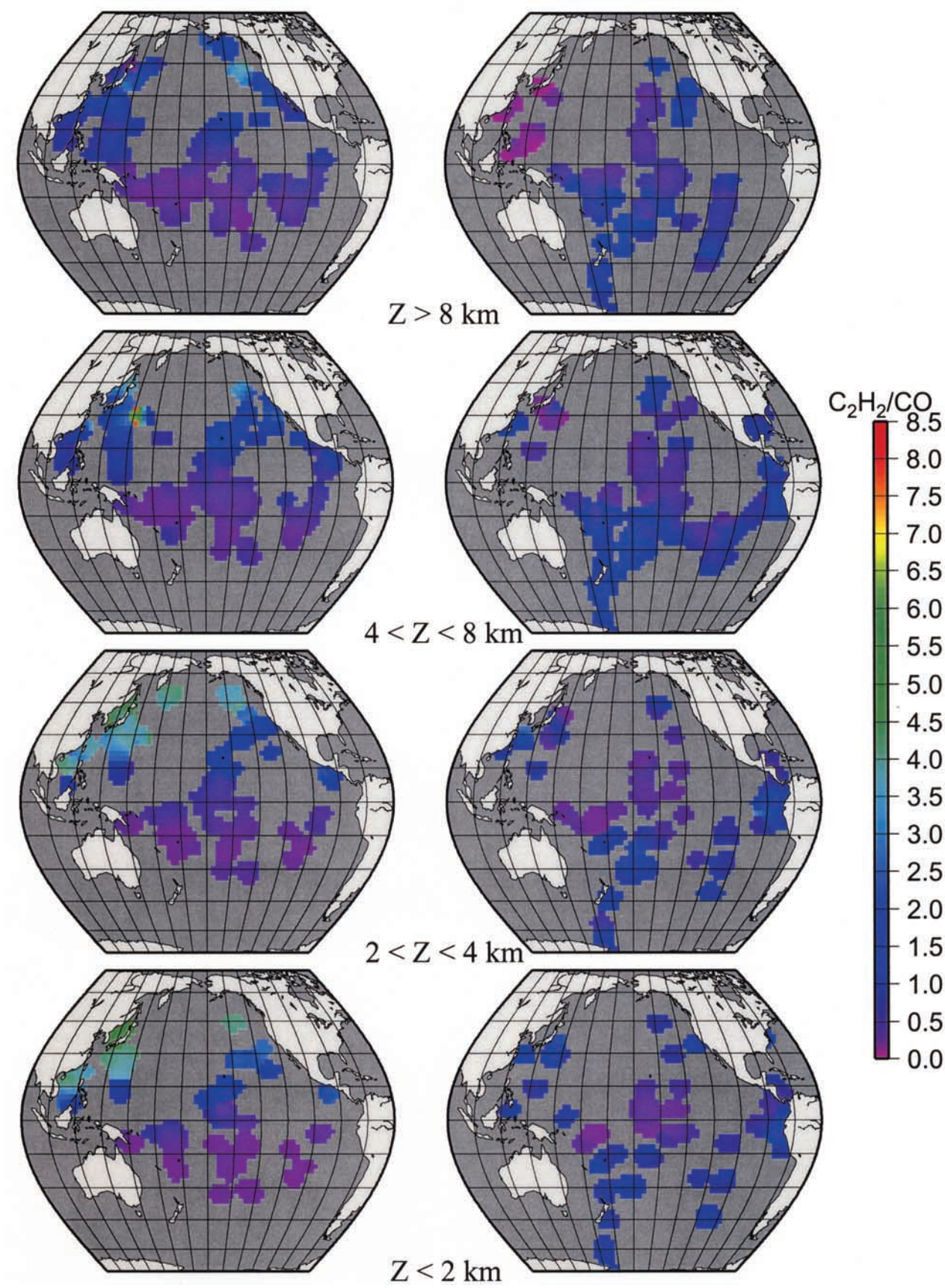

Figure 6. The ratio of ethyne (parts per trillion by volume) to CO (parts per billion by volume) in the troposphere over the Pacific during the (left) spring (PWB and PTB) and (right) fall (PWA and PTA) as a function of altitude.

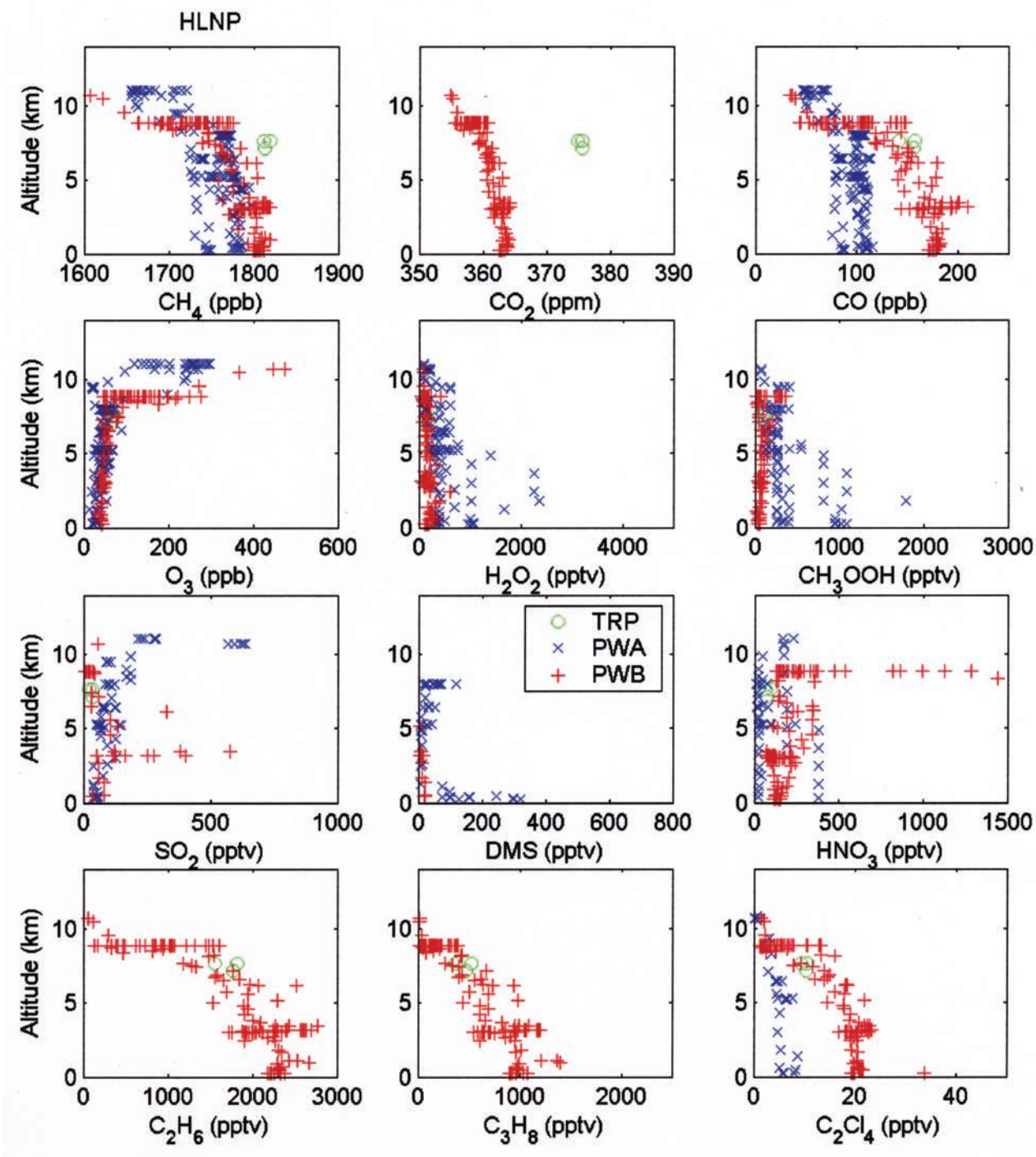

Figure 7. Altitude dependence of species mixing ratios in the high-latitude north Pacific region. Data for PWA, PWB, and TRP were available for this region.

methane increase is less now than at the beginning of the study [*Blake and Rowland*, 1988; *Simpson et al.*, 2002].

[21] The mean CH_4 and CO_2 mixing ratios for each region during the different field programs are presented in Table 2 and Figure 10. Methane is increasing over the time period of observations in all regions where there were observations in more than two field programs. The annual rate of increase is greatest in the HLNP region at 8.49 ± 1.66 ppbv yr^{-1}, with $r^2 = 0.96$, followed by the EQWP at 6.76 ± 1.78 ppbv yr^{-1}, with $r^2 = 0.83$; MSWP at 6.07 ± 2.78 ppbv yr^{-1}, with $r^2 = 0.83$; MNWP at 5.88 ± 0.37 ppbv yr^{-1}, with $r^2 = 0.99$; and the lowest in the MNEP at 4.73 ± 1.34 ppbv yr^{-1}, with $r^2 = 0.81$. In all regions the annual rate of increase is substantially lower than 0.9% observed during the 1980s, which would be about 15 ppbv yr^{-1}. *Bartlett et al.* [2003] derive a global background methane increase of 38 ± 6 ppbv between the PWB and TRP missions using methane measurements on clean air samples at Climate Monitoring and Diagnostics Laboratory (CMDL) sites for latitudes <30°N. Considering the 7-year difference between missions, this results in a background

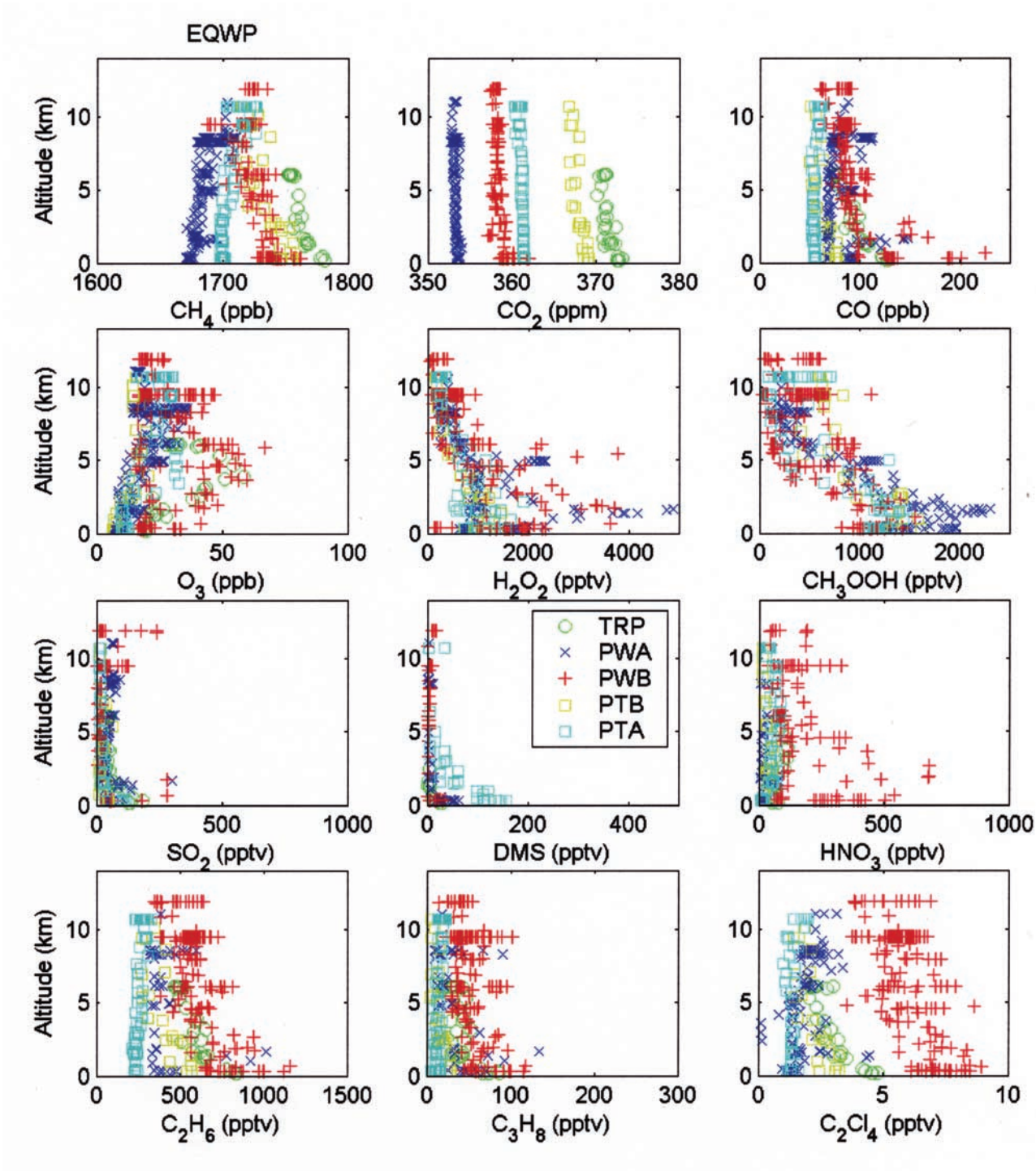

Figure 8. Altitude dependence of species mixing ratios in the equatorial western Pacific region. Data for PWA, PWB, PTA, PTB, and TRP were available for this region.

annual increase of 5.4 ± 0.9 ppbv yr^{-1} for methane for latitudes <30°N. A similar approach to calculating a global background increase using CMDL sites above 30°N results in an annual increase of 3.9 ± 1.7 ppbv yr^{-1} for methane. The regional annual rate of increase for methane is not significantly different from the global background increase for the EQWP, MSWP, MNWP, and the MNEP regions. Methane's annual rate of increase significantly exceeds the high-latitude background CMDL derived rate in the HLNP region. *Streets et al.* [2003] estimated a +6.4% increase in east Asian methane anthropogenic emission from 1994 to 2000. Increasing direct anthropogenic methane emissions from east Asia into the MNWP region do not appear to be enhancing the rate of methane increase beyond the global background rate. In the HLNP the rate of change in methane levels exceeds the expected background increase substantially, indicating the presences of a substantial source of methane to the region. *Bartlett et al.* [2003] examined the latitudinal

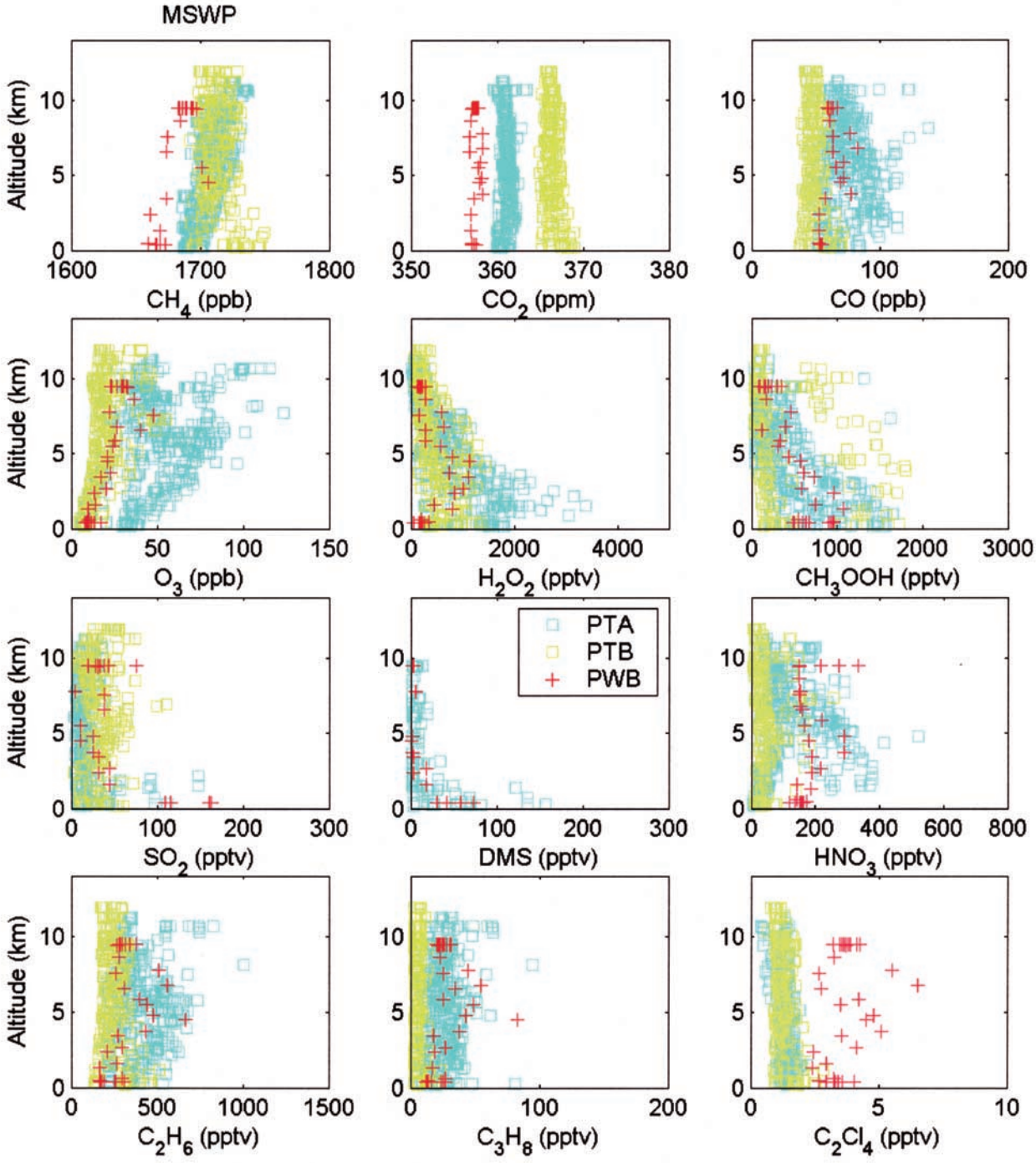

Figure 9. Altitude dependence of species mixing ratios in the midlatitude southwestern Pacific region. Data for PWB, PTA, and PTB were available for this region.

distribution of methane from the TRP program noting the largest differences between CMDL background levels are in the western Pacific between 15° and 20°N and 30° and 35°N, the northern most sampling during TRP. Elevated methane levels were also observed at these latitudes in the central Pacific at altitudes above 6 km, associated with rapid transport of continental emissions at altitude by the Japan Jet [*Bartlett et al.*, 2003]. This transport mechanism may be contributing to the enhanced rate of methane increase in the HLNP over the decade.

[22] For CO_2 the average increase in all regions is 1.92 ppmv yr^{-1}, with the MNWP exhibiting the largest rate of increase, 2.16 ± 0.11 ppmv yr^{-1}, followed by the MNEP at 2.02 ± 0.22 ppmv yr^{-1}, with $r^2 = 0.97$; EQWP at 1.84 ± 0.10 ppmv yr^{-1}, with $r^2 = 0.99$; HLNP at 1.82 ± 0.06 ppbv yr^{-1}, with $r^2 = 0.99$; and the lowest in the MSWP at 1.78 ± 0.01 ppmv yr^{-1}, with $r^2 = 1.00$. The global average increase in CO_2 during the 1990s is 0.40% yr^{-1}, which is about 1.42 ppmv yr^{-1} [*Intergovernmental Panel on Climate Change*, 1995]. The MSWP region exhibits a rate of increase

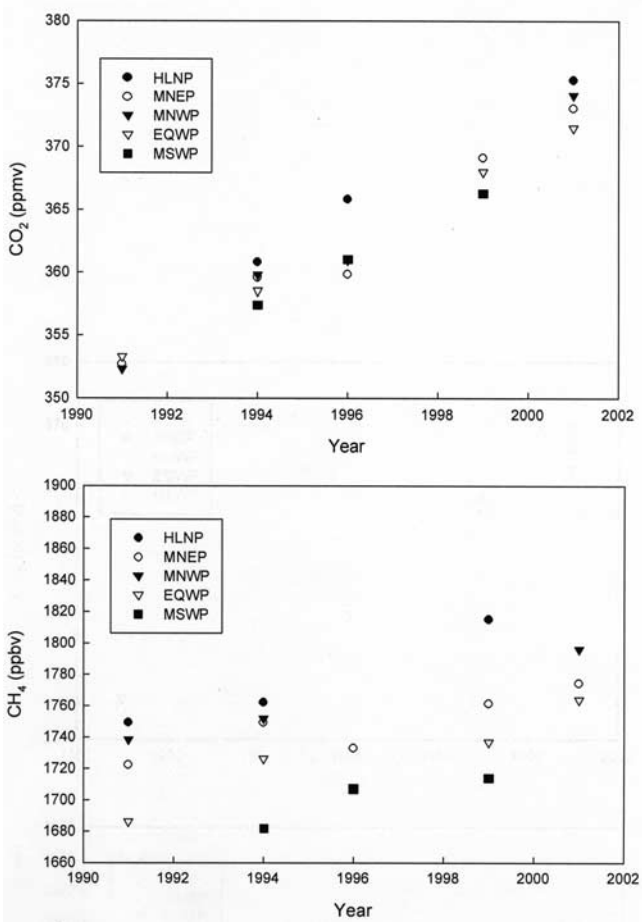

Figure 10. Average mixing ratio for CO_2 and CH_4 in the various regions during the GTE field campaigns.

that is the most similar to the global average. The MNEP and MNWP exceed the global average rate of increase by 42% and 52%, respectively. The vertical distribution of CO_2 is presented for each region in Figures 7, 8, 9, 11, and 12. Methane exhibits a lower altitude (<6–8 km) surface enhancement in most regions, a surface enhancement is not as evident for CO_2 but is present with a low-altitude enhancement of 2–3 ppmv in areas influenced by Asian outflow. The annual increase in CO_2 loading is evident in these plots at all altitudes. The vertical gradient is also evident as a general decrease in CO_2 mixing ratio with altitude. The most pronounced near surface elevation in CO_2 is consistently observed in the MNWP region. *Vay et al.* [2003] examined the latitudinal and longitudinal distribution of CO_2 during the TRP mission and found a band of maximum emission between 35° and 40°N, with a strong linear relationship between CO_2 emissions and latitude in the lower troposphere from 5° to 40°N. These data indicate that Asian regional emissions of CO_2 are contributing to an enhanced rate of CO_2 increase in the MNWP and MNEP regions.

3.3. SO_2 and Peroxides, Contrast Between PWB and TRP

[23] The PWB field program took place from 7 February to 15 March 1994; sampling during the TRP program took place from 23 February to 9 April 2001. *Fuelberg et al.* [2003] show that during TRP there was a shift in meteorological conditions from winter to spring and describe the flow patterns associated with these two regimes. A description of the meteorological conditions prevalent during PWB is given by *Merrill et al.* [1997]. *Fuelberg et al.* [2003] compared the streamlines derived from mission-averaged winds throughout the troposphere, precipitation patterns, and the frequency and intensity of midlatitude cyclones for TRP and PWB. Their analysis has demonstrated that the meteorological conditions were quite similar during the two missions. *Dibb et al.* [2003] examined the SSMI rainfall products and GPCP precipitation anomaly fields for eastern Asia and the western Pacific for the two field programs and did not find any persistent differences. The similarity in mission time, overall meteorology, precipitation, and sampling locations present a unique opportunity to examine long-term changes in species mixing ratios.

[24] It is possible to compare the mean peroxide mixing ratios between the two missions in only three regions, the HLNP, MNEP, and MNWP. The mean mixing ratio for H_2O_2 is similar in the HLNP, although there are a limited number of samples to base the comparison on during TRP in the HLNP region. The increase for TRP in the MNEP of 273 pptv is significant at the 99% confidence level. Sampling in the MNWP produced a large number of observations in both missions, and PWB exhibits higher H_2O_2 levels, 670 pptv compared to 614 pptv during TRP, this difference is significant at the 85% confidence level (Table 2). For CH_3OOH the levels have increased in all three regions for TRP. The increase in the HLNP is not statistically significant, but for the MNEP and MNWP, the observations during TRP are 2.5 times and 12% higher than during PWB, respectively. These differences are significant at the 99% and 95% confidence levels, respectively. Increases in CH_3OOH levels would be expected as methane levels increase, since methane oxidation is the primary source of CH_3OOH over oceanic waters [*Lee et al.*, 2000]. Vertical profiles of H_2O_2 and CH_3OOH exhibit a maximum ≈2 km (usually right above the cloud tops), with decreasing concentrations with increasing altitude, and lower concentrations in the boundary layer [*Lee et al.*, 2000]. The vertical profile of H_2O_2 mixing ratio in 1 km altitude bins in the MNWP is shown in Figure 13 for both PWB and TRP missions. In PWB, H_2O_2 exhibits the typical vertical profile; however, in TRP in the MNWP the maximum at 2 km has been eliminated. This is not the case for CH_3OOH which exhibits a typical profile in both programs (not shown).

[25] The levels of SO_2 in the MNEP, MNWP, and EQWP regions were 2.5–3 times higher during TRP than during PWB (Table 2). The observed differences for SO_2 in the MNEP are not significant; for the MNWP and EQWP the differences are significant at the 99% confidence level. M. Kim et al. (Trends in SO_2 over the west Pacific: Comparison of TRACE-P and PEM West B, unpublished manuscript, 2003) have examined the distribution of SO_2 during the TRP program and found the greatest differences between the TRP and PWB mission in the 1- to 3-km altitude range (Figures 11 and 12). The average and median mixing ratios for SO_2 in 1 km altitude bins are shown in Figure 13 for the MNWP region for both TRP and PWB programs. Average mixing ratios of SO_2 are significantly larger in TRP at altitudes below 4 km in this region (Figure 13).

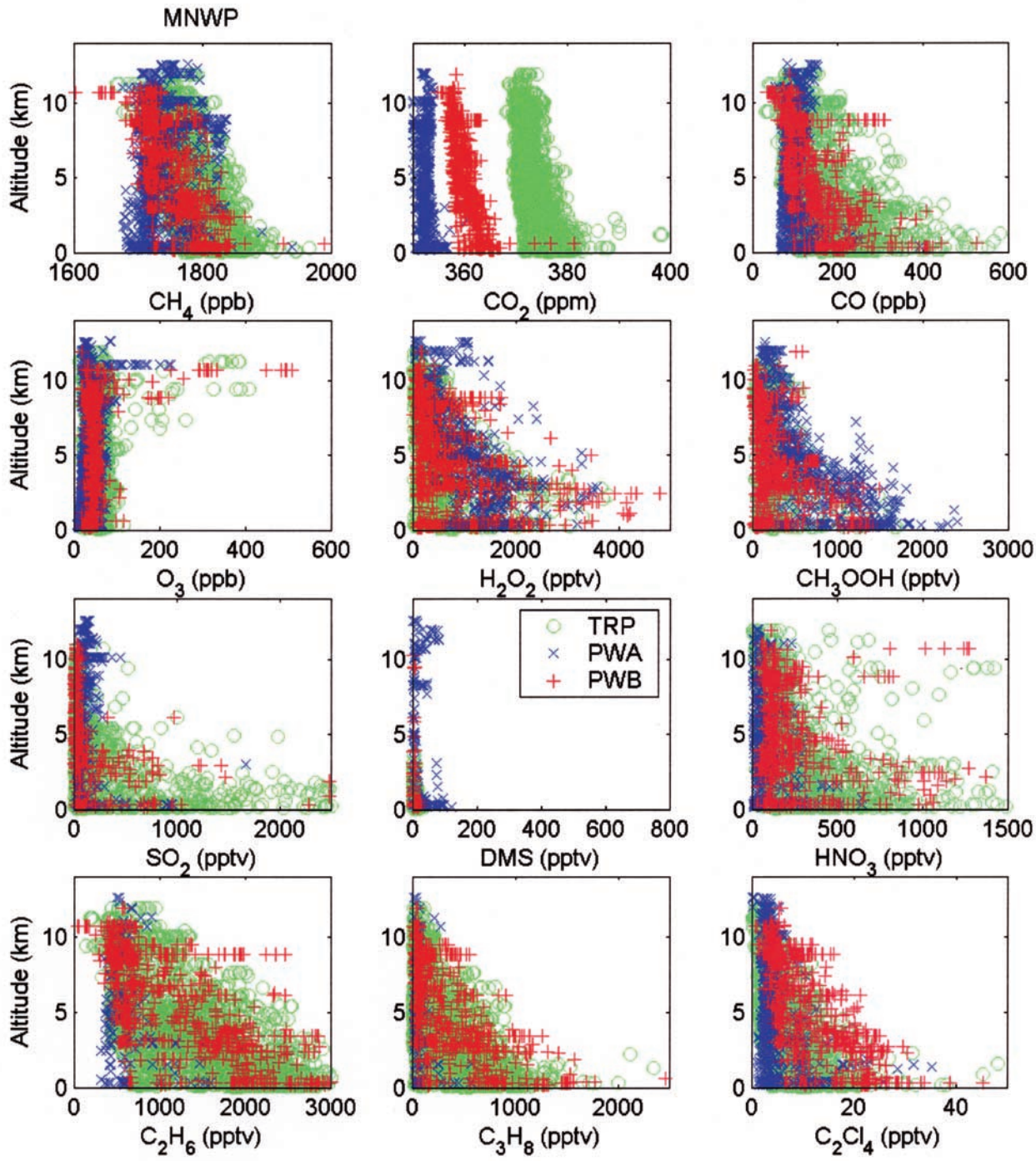

Figure 11. Altitude dependence of species mixing ratios in the midlatitude northwestern Pacific region. Data for PWA, PWB, and TRP were available for this region.

[26] Observations from both programs that had been impacted by local volcanic emissions were removed from the computations. The increased levels of SO_2 are in contrast to the recent estimation of a 17% reduction in east Asian anthropogenic SO_2 emissions between 1994 and 2000 [*Streets et al.*, 2003]. Non-sea-salt sulfate is also elevated during TRP in this region, particularly in the lowest altitude range (Figure 13). Although continental anthropogenic emissions have decreased, there is a clear increase in SO_2 levels. The origin of the SO_2 is unclear but may reflect increased shipping activity and/or nonpoint source volcanic emissions in the region. Recently, *Davis et al.* [2001] have shown ship emissions can significantly affect boundary layer SO_2 levels in the North Pacific. Unfortunately, the absence of observations between the programs precludes determining whether the increased SO_2 levels represent a secular change. We believe enhanced sulfur loading in the MNWP and other regions appears to have lead to a suppression of H_2O_2 mixing ratios relative to that of CH_3OOH. The levels of SO_2 and non-sea-salt sulfate

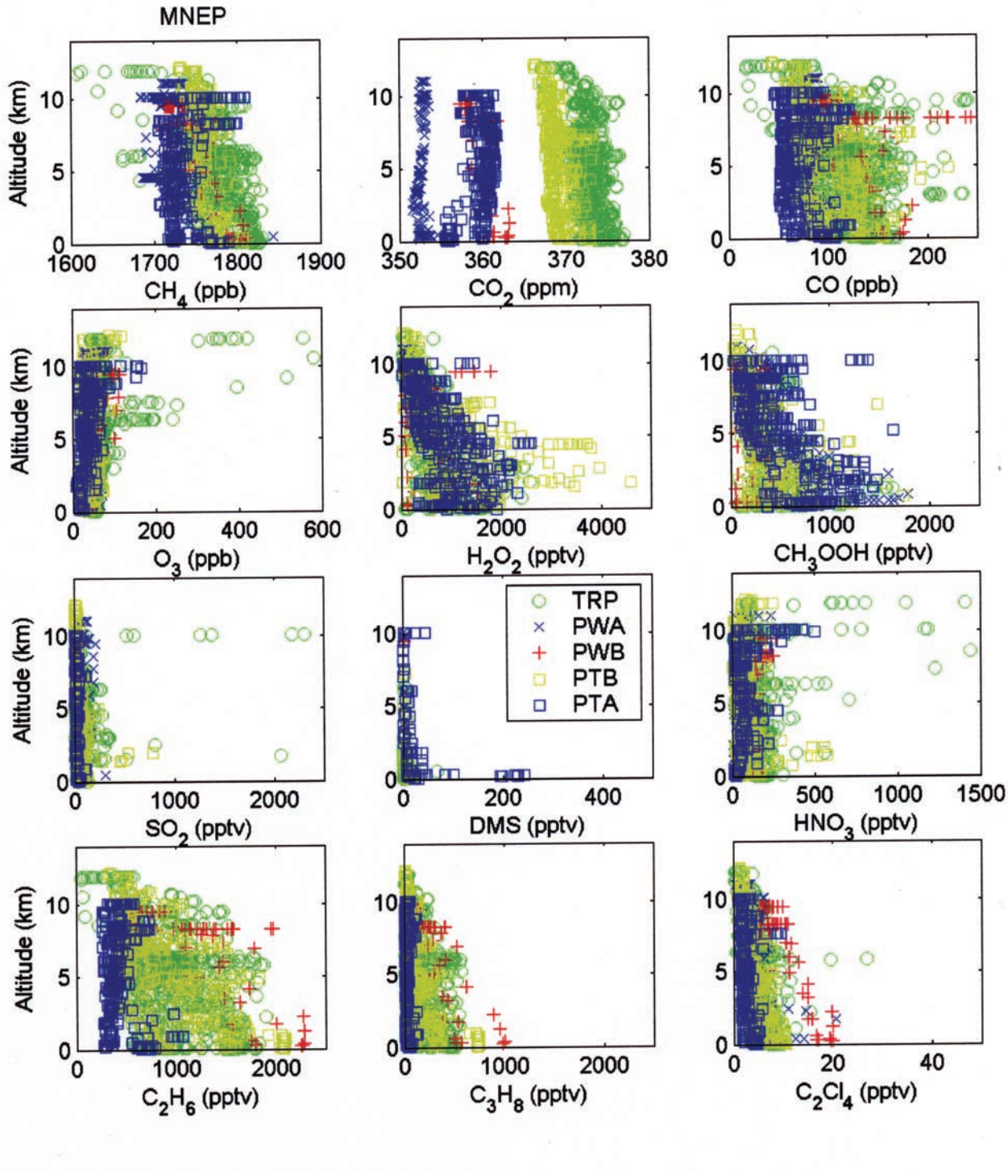

Figure 12. Altitude dependence of species mixing ratios in the midlatitude northeastern Pacific region. Data for PWA, PWB, PTA, PTB, and TRP were available for this region.

observed during the TRP program are sufficient to reduce H_2O_2 levels by 500 to 700 pptv. Transport of boundary layer SO_2 at the levels observed during TRP vertically through the marine boundary layer could remove the typical cloud top H_2O_2 maximum.

[27] There are several other possible explanations for lower H_2O_2 levels during TRP. First, lower H_2O_2 levels could be due to a suppression of HO_2 levels as a result of higher NO levels in the regions during TRP. The regional mean NO mixing ratios are not substantially different between TRP and PWB; however, the range of observed levels was much larger during TRP in the MNEP and MNWP. *Davis et al.* [2003] have shown that the levels of HO_2 were generally a factor of 2 higher during TRP than

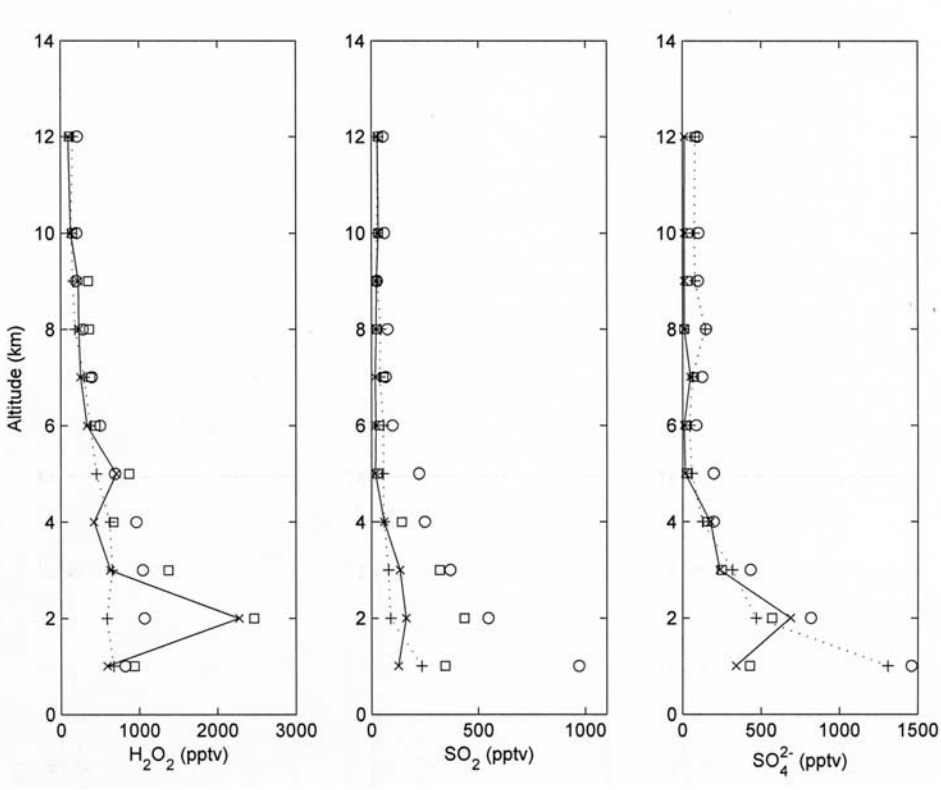

Figure 13. Vertical profiles of the average (TRP (circle) and PWB (square)) and median (TRP (plus sign) and PWB (cross)) mixing ratios for SO_2, H_2O_2, and non-sea-salt sulfate. SO_2 measurements that were impacted by volcanic emissions in PWB and TRP have been excluded from the average and median calculations.

PWB. Consequently, suppression of HO_2 via NO during TRP does not appear to be responsible for lower H_2O_2 levels. In the absence of a removal process for H_2O_2, the high HO_2 levels would result in increased levels of H_2O_2. A second possibility is that the three week shift in sampling time between missions could account for the lower levels due to a decrease in photochemical activity for the TRP period. *Davis et al.* [2003] show that in addition to HO_2, levels of OH and $J(O^1D)$ were nearly a factor of 2 larger during TRP than PWB. They conclude that the shifts in these species were largely due to the 3-week change in solar zenith angle and increasing UV actinic flux. All of this points to an enhanced level of photochemistry during TRP, which should result in higher levels of H_2O_2.

[28] A third possible cause of lower H_2O_2 levels could be enhanced scavenging, if the atmosphere was scavenged more efficiently by precipitation during TRP relative to PWB in the MNWP region. *Fuelberg et al.* [2003] compared the precipitation fields between PWB and TRP and found no differences. *Dibb et al.* [2003] examined several rainfall products and did not find precipitation differences between missions over the western Pacific. Further evidence against an enhanced scavenging explanation for lower H_2O_2 levels can be found by considering other water-soluble species. A comparison of the NO_y species between PWB and TRP by *Talbot et al.* [2003] indicate the levels of HNO_3 and PAN were 2–5 times higher during TRP in the boundary layer over the northwestern Pacific than during PWB. The mean mixing ratio of HNO_3 in the MNWP during PWB and TRP were 258 ± 467 and 274 ± 344 pptv, respectively (Table 2). The similarity between the regional mean mixing ratios supports a similar scavenging environment between missions. *Talbot et al.* [2003] has shown up to a fivefold increase in HNO_3 in the lower troposphere in coastal air masses during TRP; HNO_3 levels at altitudes >5 km are not substantially different between missions (Figure 11). These levels in the boundary layer and lower troposphere suggest that precipitation scavenging is not responsible for the lower H_2O_2 mixing ratios, since HNO_3 and other soluble species would also be removed. *Dibb et al.* [2003] have shown a significant increase in the mixing ratios of water-soluble aerosol species during TRP compared to PWB in this region. These observations support the assertion that the lower H_2O_2 mixing ratios are driven by gas phase or aerosol chemical suppression rather than enhanced wet deposition during TRP. *Browell et al.* [2003] show a much stronger boundary layer aerosol outflow for TRP relative to PWB, and *Dibb et al.* [2003] have shown a larger dust aerosol component during TRP. We believe the elevated levels of SO_2 coupled with increased aerosol surface in the lower troposphere during TRP have resulted in the suppression of H_2O_2 in the lower troposphere in the MNWP region. Levels of CH_3OOH would not be as strongly influenced by this mechanism since CH_3OOH is not as soluble as H_2O_2 in aqueous phases [*O'Sullivan et al.*, 1996]. Reduction of H_2O_2 levels through heterogeneous reaction with SO_2 and its conversion to non-sea-salt sulfate results in changes of 500–1000 pptv for these species. Since all the GTE programs focused on gas phase

chemistry, cloud process were not directly observed. However, we believe the MNWP observations from TRP present a compelling example of a regional scale heterogeneous loss of H_2O_2 by reaction with SO_2.

4. Conclusions

[29] Data from five NASA-GTE missions were examined to identify long-term and seasonally driven changes in the distribution of hydrogen peroxide, methylhydroperoxide, and selected species in the Pacific troposphere. During the most recent missions, PEM Tropics B and TRP, H_2O_2 and CH_3OOH were measured from the NASA DC-8 and P3-B during February–April 1999 and 2001, respectively. Over the last decade, flights on the two aircraft sampled the Pacific troposphere at altitudes from 0.5 km to 13 km and from 130°E to 115°W and from about 65°N to 70°S. The Pacific troposphere was subdivided into eight different geographic regions where long-term trends and seasonal changes in the observed species mixing ratios were examined as a function of altitude. Changes in species mixing ratios are discussed with respect to changes in source, transport, and photochemical production and loss process over the decade. Only long-lived atmospheric species exhibited monotonic annual trends; CH_4 and CO_2 exhibited average annual mixing ratio increases of 6.39 ppbv yr^{-1} and 1.92 ppmv yr^{-1}, respectively. Methane exhibited the greatest annual rate of increase in the HLNP region at 8.49 ppbv yr^{-1}, followed by the EQWP. For CO_2 the MNWP exhibited the largest rate of increase, 2.16 ppmv yr^{-1}, with the MSWP having the lowest rate of increase, 1.78 ppmv yr^{-1}. O_3, CO, and NO all exhibit significantly higher mixing ratios in the north Pacific troposphere in the spring relative to the fall, but these species did not exhibit a clear annual trend. H_2O_2 mixing ratios were 38 ± 16% higher [Δ(fall-spring)258 ± 34 pptv], and CH_3OOH was 61 ± 15% higher (Δ343 ± 76 pptv) throughout the Pacific troposphere in the fall than in the spring. The distribution of the peroxides is greatly influenced by seasonal changes in transport and photochemical production and loss. Elevated levels of peroxides associated with Asian outflow are most pronounced during the spring in the western Pacific. Injection of peroxides into the upper troposphere is evident at the ITCZ in fall and near the SPCZ during the spring. SO_2 loading in the north Pacific lower troposphere was 2–3 times larger during 2001 than during earlier years, in contrast to a 17% reduction in continental anthropogenic east Asian SO_2 emissions estimated by *Streets et al.* [2003]. Other species that are good tracers of anthropogenic emission sources, C_2H_6, C_3H_8, and C_2H_2, do not exhibit significant increases in their average mixing ratios during 2001, and C_2Cl_4 appears to be decreasing. CH_3I, a tracer for oceanic emission, also does not exhibit an increase in 2001. Consequently, the cause for the increased SO_2 loading is unclear. However, the enhanced sulfur loading appears to have resulted in a suppression of H_2O_2 mixing ratios throughout the midlatitude north Pacific troposphere. Other processes that could lead to lower H_2O_2 mixing ratios do not appear to be responsible for the decrease.

[30] **Acknowledgments.** This research was supported by the National Aeronautics and Space Administration Global Tropospheric Experiment with awards to B.G.H. at the University of Rhode Island and D.W.O. at the United States Naval Academy. This project was successful as a result of the excellent scientific and logistical support offered by Joe McNeal, Jim Hoell, Jim Raper, Vicki Connors, and the SAIC project office, respectively. We would also like to thank the crew and support staff of the DC-8 and P-3B for many eventful and uneventful flight operations. This manuscript was improved as a result of the thoughtful comments offered by three reviewers for which we are thankful.

References

Ayers, G. P., S. A. Penkett, R. W. Gillett, B. Bandy, I. E. Galbally, C. P. Meyer, C. M. Elsworth, S. T. Bently, and B. W. Forgan (1992), Evidence for photochemical control of ozone concentrations in unpolluted marine air, *Nature*, *360*, 446–449.

Ayers, G. P., S. A. Penkett, R. W. Gillett, B. Bandy, I. E. Galbally, C. P. Meyer, C. M. Elsworth, S. T. Bently, and B. W. Forgan (1996), The annual cycle of peroxides and ozone in marine air at Cape Grim, Tasmania, *J. Atmos. Chem.*, *23*, 221–252.

Bachmeier, S. A., and H. J. Fuelberg (1996), A meteorological overview of the TRACE A period, *J. Geophys. Res.*, *101*, 23,881–23,888.

Bartlett, K. B., G. W. Sachse, T. Slate, C. Harward, and D. R. Blake (2003), Large-scale distribution of CH_4 in the western Pacific: Sources and transport from the Asian continent, *J. Geophys. Res.*, *108*(D20), 8807, doi:10.1029/2002JD003076.

Blake, D. R., and F. S. Rowland (1988), Continuing worldwide increase in tropospheric methane, *Science*, *239*, 1129–1131.

Blake, D. R., T.-Y. Chen, T. W. Smith Jr., C. J.-L. Wang, O. W. Wingenter, N. J. Blake, F. S. Rowland, and E. W. Mayer (1996), Three-dimensional distribution of NMHCs and halocarbons over the northwestern Pacific during the 1991 Pacific Exploratory Mission (PEM-West A), *J. Geophys. Res.*, *101*, 1763–1778.

Blake, N. J., et al. (2003), NMHCs and halocarbons in Asian continental outflow during the Transport and Chemical Evolution over the Pacific (TRACE-P) field campaign: Comparison with PEM-West B, *J. Geophys. Res.*, *108*(D20), 8806, doi:10.1029/2002JD003367.

Bradshaw, J., et al. (1999), Photofragmentation two-photon laser-induced detection of NO_2 and NO: Comparison of measurements with model results based on airborne observations during PEM-Tropics A, *Geophys. Res. Lett.*, *26*, 471–474.

Browell, E. V., et al. (1996), Large-scale air mass characteristics observed over western Pacific during summertime, *J. Geophys. Res.*, *101*, 1691–1712.

Browell, E. V., et al. (2003), Large-scale ozone and aerosol distributions, air mass characteristics, and ozone fluxes over the western Pacific Ocean in late winter/early spring, *J. Geophys. Res.*, *108*(D20), 8805, doi:10.1029/2002JD003290.

Cicerone, R., and R. Oremland (1988), Biogeochemical aspects of atmospheric methane, *Global Biogeochem. Cycles*, *2*, 299–327.

Claiborn, C. S., and V. P. Aneja (1991), Measurements of atmospheric hydrogen peroxide in the gas phase and in cloud water at Mt. Mitchell, North Carolina, *J. Geophys. Res.*, *96*, 18,771–18,787.

Clark, A. D., W. G. Collins, P. J. Rasch, V. N. Kapustin, K. Moore, S. Howell, and H. E. Fuelberg (2001), Dust and pollution transport on global scales: Aerosol measurements and model predictions, *J. Geophys. Res.*, *106*, 32,555–32,569.

Cohan, D. S., M. G. Schultz, D. J. Jacob, B. G. Heikes, and D. R. Blake (1999), Convective injection and photochemical decay of peroxides in the upper troposphere, *J. Geophys. Res.*, *104*, 5717–5724.

Davis, D. D., G. Grodzinsky, P. Kasibhatla, J. Crawford, G. Chen, S. Liu, A. Bandy, D. Thornton, H. Guan, and S. Sandholm (2001), Impact of ship emissions on marine boundary layer NO_x and SO_2 distributions over the Pacific basin, *Geophys. Res. Lett.*, *28*, 235–238.

Davis, D. D., et al. (2003), An assessment of western North Pacific ozone photochemistry based on springtime observations from NASA's PEM-West B (1994) and TRACE-P (2001) field studies, *J. Geophys. Res.*, *108*(D21), 8829, doi:10.1029/2002JD003232.

Dibb, J. E., R. Talbot, E. Scheuer, G. Seid, M. Avery, and H. Singh (2003), Aerosol chemical composition in Asian continental outflow during TRACE-P campaign: Comparison with PEM-West B, *J. Geophys. Res.*, *108*(D21), 8815, doi:10.1029/2002JD003111.

Fels, M., and W. Junkermann (1994), The occurrence of organic peroxides in air at a mountain site, *Geophys. Res. Lett.*, *21*, 341–344.

Fuelberg, H. E., R. E. Newell, S. P. Longmore, Y. Zhu, D. J. Westberg, E. V. Browell, D. R. Blake, G. L. Gregory, and G. W. Sachse (1999), A meteorological overview of the Pacific Exploratory Mission (PEM) Tropics period, *J. Geophys. Res.*, *104*, 5585–5622.

Fuelberg, H. E., R. E. Newell, D. J. Westberg, J. C. Maloney, J. R. Hannan, B. D. Martin, M. A. Avery, and Y. Zhu (2001), A meteorological overview of the second Pacific Exploratory Mission in the Tropics, *J. Geophys. Res.*, *106*(D23), 32,427–32,443.

Fuelberg, H. E., C. M. Kiley, J. R. Hannan, D. J. Westberg, M. A. Avery, and R. E. Newell (2003), Meteorological conditions and transport pathways during the Transport and Chemical Evolution over the Pacific (TRACE-P) experiment, *J. Geophys. Res.*, *108*(D20), 8782, doi:10.1029/2002JD003092.

Gregory, G. L., et al. (1999), Chemical characteristics of Pacific tropospheric air in the region of the Intertropical Convergence Zone and South Pacific Convergence Zone, *J. Geophys. Res.*, *104*, 5677–5696.

Gunz, D. W., and M. R. Hoffmann (1990), Atmospheric chemistry of peroxides: A review, *Atmos. Environ., Part A*, *24*, 1601–1633.

Heikes, B. G. (1992), Formaldehyde and hydroperoxides at Mauna Loa Observatory, *J. Geophys. Res.*, *97*, 18,001–18,013.

Heikes, B. G., M. Lee, J. Bradshaw, S. Sandholm, D. D. Davis, W. Chameides, H. Rodriguez, S. Liu, and S. McKeen (1996), Hydrogen peroxide and methylhydroperoxide distributions related to ozone and odd hydrogen over the North Pacific in the fall of 1991, *J. Geophys. Res.*, *101*, 1891–1905.

Hewitt, C. N., and G. L. Kok (1991), Formation and occurrence of organic peroxides in the troposphere: Laboratory and field observations, *J. Atmos. Chem.*, *12*, 181–194.

Hoell, J. M., D. D. Davis, S. C. Liu, R. E. Newell, H. Akimoto, R. J. McNeal, and R. J. Bendura (1997), The Pacific Exploratory Mission-West Phase B: February–March 1994, *J. Geophys. Res.*, *102*, 28,223–28,239.

Intergovernmental Panel on Climate Change (1995), *Climate Change, 1994: Radiative Forcing of Climate Change and an Evaluation of the IPCC IS92 Emission Scenarios*, edited by J. T. Houghton et al., Cambridge Univ. Press, New York.

Jacob, D. J., L. W. Horowitz, J. W. Munger, B. G. Heikes, R. R. Dickerson, R. S. Artz, and W. C. Keene (1995), Seasonal transition from NO_x – to hydrocarbon-limited conditions for ozone production over the eastern United States in September, *J. Geophys. Res.*, *100*, 9315–9324.

Jacob, D. J., J. H. Crawford, M. M. Kleb, V. S. Connors, R. J. Bendura, J. L. Raper, G. W. Sachse, J. C. Gille, L. Emmons, and C. L. Heald (2003), Transport and chemical evolution over the Pacific (TRACE-P) aircraft mission: Design, execution, and first results, *J. Geophys. Res.*, *108*(D20), 9000, doi:10.1029/2002JD003276.

Kok, G. L., S. E. McLaren, and T. A. Staffelbach (1995), HPLC determination of atmospheric organic hydroperoxides, *J. Atmos. Oceanic Technol.*, *12*, 282–289.

Lashof, D. A., and D. R. Ahuja (1990), Relative contributions of greenhouse gas emissions to global warming, *Nature*, *344*, 529–531.

Lazrus, A. L., G. L. Kok, J. A. Lind, S. N. Gitlin, B. G. Heikes, and R. E. Shetter (1986), Automated fluorometric determination of hydrogen peroxide vapor in air, *Anal. Chem.*, *58*, 5594–5597.

Lee, J. H., D. F. Leahy, I. N. Tang, and L. Newman (1993), Measurement and speciation of gas phase peroxides, *J. Geophys. Res.*, *98*, 2911–2915.

Lee, M., D. O'Sullivan, K. B. Noone, and B. G. Heikes (1995), HPLC method for the determination of H_2O_2, C_1 and C_2 hydroperoxides in the atmosphere, *J. Atmos. Oceanic Technol.*, *12*, 1060–1070.

Lee, M., B. G. Heikes, and D. W. O'Sullivan (2000), Hydrogen peroxide and organic hydroperoxide in the troposphere: A review, *Atmos. Environ.*, *34*, 3475–3494.

McDonald, A. M., K. G. Anlauf, C. M. Banic, W. R. Leaitch, and H. A. Wiebe (1995), Airborne measurements of aqueous and gaseous hydrogen peroxide during spring and summer in Ontario, Canada, *J. Geophys. Res.*, *100*, 7253–7262.

Merrill, J. T., R. E. Newell, and A. S. Bachmeier (1997), A meteorological overview for the Pacific Exploratory Mission-West Phase B, *J. Geophys. Res.*, *102*, 28,241–28,253.

Olson, J. R., et al. (2001), Seasonal differences in the photochemistry of the South Pacific: A comparison of observations and model results from PEM-Tropics A and B, *J. Geophys. Res.*, *106*, 32,749–32,766.

Olszyna, K. J., J. F. Meagher, and E. M. Bailey (1988), Gas-phase, cloud and rain-water measurements of hydrogen peroxide at a high-elevation site, *Atmos. Environ.*, *22*, 1699–1706.

O'Sullivan, D. W., M. Lee, B. C. Noone, and B. G. Heikes (1996), Henry's law constant determinations for hydrogen peroxide, methyl hydroperoxide, hydroxymethyl hydroperoxide, ethyl hydroperoxide, and peroxyacetic acid, *J. Phys. Chem.*, *100*, 3241–3247.

O'Sullivan, D. W., B. G. Heikes, M. Lee, W. Chang, G. L. Gregory, D. R. Blake, and G. W. Sachse (1999), Distribution of hydrogen peroxide and methylhydroperoxide over the Pacific and South Atlantic Oceans, *J. Geophys. Res.*, *104*, 5635–5646.

Prather, M. J., and D. J. Jacob (1997), A persistent imbalance in HO_x and NO_x photochemistry of the upper troposphere driven by deep tropical convection, *Geophys. Res. Lett.*, *24*, 3189–3192.

Raper, J. L., M. M. Kleb, D. J. Jacob, D. D. Davis, R. E. Newell, H. E. Fuelberg, R. J. Bendura, J. M. Hoell, and R. J. McNeal (2001), Pacific Exploratory Mission in the tropical Pacific: PEM-Tropics B, March–April 1999, *J. Geophys. Res.*, *106*(D23), 32,401–32,425.

Sachse, G. W., G. F. Hill, W. L. Wade, and M. G. Perry (1987), Fast-response, high-precision carbon monoxide sensor using a tunable diode laser absorption technique, *J. Geophys. Res.*, *92*, 2071–2081.

Sachse, G. W., J. E. Collins, G. F. Hill, L. O. Wade, L. G. Burney, and J. A. Ritter (1991), Airborne tunable diode laser sensor for high precision concentration and flux measurements of carbon monoxide and methane, *Proc. SPIE Int. Soc. Opt. Eng.*, *1433*, 145–156.

Sakugawa, H., I. R. Kaplan, W. Tsai, and Y. Cohen (1990), Atmospheric hydrogen peroxide, *Environ. Sci. Technol.*, *24*, 1452–1462.

Simpson, I. J., D. R. Blake, F. S. Rowland, and T. Y. Chen (2002), Implications of the recent fluctuations in the growth rate of tropospheric methane, *Geophys. Res. Lett.*, *29*(10), 1479, doi:10.1029/2001GL014521.

Smyth, S., et al. (1996), Comparison of free tropospheric western Pacific air mass classification schemes for the PEM West A experiment, *J. Geophys. Res.*, *101*, 1743–1762.

Streets, D. G., et al. (2003), An inventory of gaseous and primary aerosol emissions in Asia in the year 2000, *J. Geophys. Res.*, *108*(D21), 8809, doi:10.1029/2002JD003093.

Talbot, R., J. E. Dibb, E. M. Scheuer, D. R. Blake, N. J. Blake, G. L. Gregory, G. W. Sachse, J. D. Bradshaw, S. T. Sandholm, and H. B. Singh (1999), Influence of biomass combustion emissions on the distribution of acidic trace gases over the southern Pacific basin during austral springtime, *J. Geophys. Res.*, *104*, 5623–5634.

Talbot, R., et al. (2003), Reactive nitrogen in Asian continental outflow over the western Pacific: Results from the Transport and Chemical Evolution over the Pacific (TRACE-P) airborne mission, *J. Geophys. Res.*, *108*(D20), 8803, doi:10.1029/2002JD003129.

Thornton, D. C., A. R. Bandy, F. H. Tu, B. W. Blomquist, G. M. Mitchell, W. Nadler, and D. H. Lenschow (2002), Fast airborne sulfur dioxide measurements by Atmospheric Pressure Ionization Mass Spectrometry (APIMS), *J. Geophys. Res.*, *107*(D22), 4632, doi:10.1029/2002JD002289.

Tremmel, H. G., W. Junkermann, F. Slemr, and U. Platt (1993), On the distribution of hydrogen peroxide in the lower troposphere over the northeastern United States during late summer 1988, *J. Geophys. Res.*, *98*, 1083–1099.

Tremmel, H. G., W. Junkermann, and F. Slemr (1994), Distribution of organic peroxides during aircraft measurements over the northeastern United States, *J. Geophys. Res.*, *99*, 5295–5307.

Vay, S., et al. (2003), The influence of regional-scale anthropogenic emissions on CO_2 distributions over the western North Pacific, *J. Geophys. Res.*, *108*(D20), 8801, doi:10.1029/2002JD003094.

Watkins, B. A., D. D. Parrish, M. Trainer, R. B. Norton, J. E. Yee, and F. C. Fehsenfeld (1995a), Factors influencing the concentration of gas phase hydrogen peroxide during the summer at Niwot Ridge, Colorado, *J. Geophys. Res.*, *100*, 22,831–22,840.

Watkins, B. A., D. D. Parrish, S. Buhr, R. B. Norton, M. Trainer, J. E. Yee, and F. C. Fehsenfeld (1995b), Factors influencing the concentration of gas phase hydrogen peroxide during the summer at Kinterbish, Alabama, *J. Geophys. Res.*, *100*, 22,841–22,851.

Weinstein-Lloyd, J., P. H. Daum, L. J. Nummermacker, J. H. Lee, and L. I. Kleinman (1996), Measurement of peroxides and related species in the 1993 North Atlantic Regional Experiment, *J. Geophys. Res.*, *101*, 29,081–29,090.

Weinstein-Lloyd, J. B., J. H. Lee, P. H. Daum, L. I. Kleinman, L. J. Nummermacker, S. R. Springston, and L. Newman (1998), Measurements of peroxides and related species during the 1995 summer intensive of the Southern Oxidants Study in Nashville, *J. Geophys. Res.*, *103*, 22,361–22,373.

Wu, Z., R. E. Newell, Y. Zhu, B. E. Anderson, E. V. Browell, G. L. Gregory, G. W. Sachse, and J. E. Collins (1997), Atmospheric layers measured from the NASA DC-8 during PEM-West B and comparison with PEM-West A, *J. Geophys. Res.*, *102*, 28,353–28,365.

M. Avery, Atmospheric Sciences Division, NASA Langley Research Center, Hampton, VA 23665, USA.

A. R. Bandy and D. C. Thornton, Department of Chemistry, Drexel University, Philadelphia, PA 19104, USA.

D. R. Blake, Department of Chemistry, University of California, Irvine, Irvine, CA 92717, USA.

P. Burrow and D. W. O'Sullivan, Chemistry Department, U.S. Naval Academy, Annapolis, MD 21402, USA. (osulliva@usna.edu)

B. G. Heikes and J. Snow, Center for Atmospheric Chemical Studies, Graduate School of Oceanography, University of Rhode Island, Narragansett, RI 02882, USA.

G. W. Sachse, NASA Langley Research Center, Hampton, VA 23665, USA.

R. W. Talbot, Institute for the Study of Earth, Oceans, and Space, University of New Hampshire, Durham, NH 03824, USA.